بسم الله الرحمن الرحيم

Sudan University for Sciences and Technology

College of Graduate Studies

Characterization of Multiple Sclerosis on the Brain Magnetic Resonance Images Using Texture Analysis

وصف التصلب المتعدد في صور المخ بالرنين المغنطيسي باستخدام تحليل الملمسي

A thesis Submitted for Partial Fulfillment of the Requirement of M.Sc. in Diagnostic Radiologic Technology

By:
Sarah Suliman Mohammed Elhassen

Supervisor:
Dr. Mohamed Elfadil Mohamed
(Associate professor)

2017

الأية:

قال تعالى:

اللَّهُ نُورُ السَّمَوَاتِ وَالْأَرْضِ مَثَلُ نُورِهِ كَمِشْكَوٰةٍ فِيهَا مِصْبَاحٌ الْمِصْبَاحُ فِي زُجَاجَةٍ الزُّجَاجَةُ كَأَنَّهَا كَوْكَبٌ دُرِّيٌّ يُوقَدُ مِن شَجَرَةٍ مُّبَٰرَكَةٍ زَيْتُونَةٍ لَّا شَرْقِيَّةٍ وَلَا غَرْبِيَّةٍ يَكَادُ زَيْتُهَا يُضِيٓءُ وَلَوْ لَمْ تَمْسَسْهُ نَارٌ نُّورٌ عَلَىٰ نُورٍ يَهْدِي اللَّهُ لِنُورِهِ مَن يَشَآءُ وَيَضْرِبُ اللَّهُ الْأَمْثَٰلَ لِلنَّاسِ وَاللَّهُ بِكُلِّ شَيْءٍ عَلِيمٌ ٣٥

صدق الله العظيم

{سورة النور الاية (35)}

DEDICATION

WITH MY LOVE AND APPRECIATION I DEDICATE THIS THESIS TO:

My GRANDMOTHER SOUL

My father: SULIMAN ALERAGI

My mother: EIGBAL MOBARAK

My sisters: TAYSEER & AMNA.

My brothers: MAHMOUD & MOHAMMED.

My all friends, family, and to all people those I love and respect

ACKNOWLEDGMENT

Abstract

Multiple Sclerosis (MS) is a chronic autoimmune inflammatory disease of the central nervous system, which can be diagnosed by magnetic resonace imaging (MRI) by evidence of multiple patches wight of scar tissue in different parts of the central nervous system on flair and T2 waightet images.This study is an analytical study, which conducted at Antalia hospital in a period from September 2016 to December 2016 with sample of 50 MR brain images for patient having multiple sclerosis and 50 MR brain images for patient having small vascular disease. the aim of this study was to characterize MS plaques in MR images using Texture analysis which facilitate patteren recognition that might not visible to human eye.

The results reveal that the MS areas were very different from the rest of the tissues on FLAIR images with accuracy of 91.2% and on T2 images with classification accuracy of 89.5 %, as well classifiction of MS plaques and SVD were very seperable, with classifiction accuracy of 100% (between both of them) on FLAIR images.

المستخلص

التصلب المتعدد في الدماغ هو مرض التهاب المناعة الذاتية المزمنة يصيب الجهاز العصبي المركزي يمكن أن يكون التشخيص عن طريق التصويربالرنين المغناطيسي والذي يظهر فيه على شكل بقع متعددة بيضاء اللون في أجزاء مختلفة من الجهاز العصبي المركزي في الصور المأخوذة على الزمن الثاني و كذلك بعد توهين اشارة السوائل. هذه الدراسة هي دراسة تحليلية وقد أجريت في مستشفى انطاليا في الفترة من سبتمبر 2016 إلى ديسمبر 2016 في عينة تتألف من 50 صورة للدماغ بالرنين المغناطيسي للمرضى مصابين بالتصلب المتعدد و كذلك 50 صورة للمرضى المصابين بمرض الأوعية الدموية الصغيرة . كان الهدف من هذه الدراسة هو , توصيف التصلب المتعدد في الدماغ في صور الرنين المغنطيسي باستخدام تحليل النسيجي للصور التي تمكن من توصيف المرض و ان كان لا يمكن رؤيتها بالعين المجردة. وكانت النتائج كالاتي: أن مناطق التصلب المتعدد كانت مختلفة جدا عن بقية الأنسجة الطبيعية في المخ في صور الزمن الثاني بعد توهين اشارة السوائل بدقة تصنيف تساوي 91.2٪ وعلى الصور الموزونة على الزمن الثاني بدقة تصنيف تساوي 89.5٪. ومقدرة علي التصنيف بين لويحات التصلب العصبي المتعدد وأمرض الشعيرات الدمويه الدقيقة بدقة تصنيف تساوي 100٪ بين كل منهما على صور الزمن الثاني بعد توهين اشارة السوائل.

LIST OF ABBREVIATIONS:

1H	Hydrogen
ADEM	Acute Disseminated Encephalomyelitis
B0	the magnetic field strength
CE	Contrast Enhanced
CIS	Clinical Isolated Syndrome
CM	Cerebral Microangipathy
CNS	Central Nerves System
CSF	Cerebro Spinal Fluid
CT	Computed Tomography
DICOM	Digital Imaging And Communication In Medicine
EPI	Echo Planer Imaging
FLAIR	Fluid Attenuation Inversion Recovery
FSE	Fast Spin Echo
GLCM	Gray Level Co-occurrence matrix
GRE	Gradient Echo
HN	Histogram Normalization
IDL	Interactive Data Language
LDA	Linear Discriminant Analysis
LR	Logistic Regression
MHz	Mega Heartez
MRI	Magnetic Resonance Imaging
MS	Multiple Sclerosis
Mz	Magnetization
NAWM	Normal Appearing White Matter
NDA	Nonlinear Discriminant Analysis
NWM	Normal White Matter
PD	Proton Density
RDA	Raw Data Analysis
RF	Redio Frequency
ROC	Receiver operating characteristic
ROI	Region Of Interest
SE	Spin Echo
SPSS	Statistical Package Social Science
SS	Single Shot
SVD	Small vessel disease
T1	T1-Weighted MR Imaging
T2	T2-Weighted MR Imaging
TIFF	Tagged Image File Format

LIST OF TABLES:

LIST OF CONTENTS:

Chapter One

Chapter One

Introduction

1.1. Introduction

Magnetic Resonance Imaging (MRI) had been used in diagnose of the central nervous system diseases such as tumors , abcesses and inflammatory diseases . it also give high resolution and good image contrast of the CNS. (Mark, 2003)

One of the diseases that affect CNS is the Multiple sclerosis (MS) which is a chronic autoimmune inflammatory disease of the central nervous system featured by the onset of multifocal white matter inflammatory foci resulting in irreversible parenchymal damage. (Alastair, 2002)

 MRI helps in the diagnosis of (MS) which requires evidence of multiple patches of scar tissue in different parts of the central nervous system and evidence of at least two separate attacks of the disease that detected by the Radiologist on both T2 and FLAIR images . it also can be evaluated using Texture analysis mothods which enabling disease characterization and quantification of disease distribution, these techniques may provide information that is not visible to human eye. (Alastair, 2002)

The aim of this theises is to characterizeof MS in MR images using Texture analysis features .which has been used in similar studies like in the study of Michoux (2015)   on it they used Texture Analysis methods on T2-Weighted MR Images to Assess Acute Inflammation in Brain MS Lesions.

1.2. Problem of the study:

Generally in radiology the pathology or any abnormality will be diagnosed by the radiologist as abnormal area depending on visual perception which is subjective and affected by many factors .this situation lead mostly some times to miss diagnosis also MS has a lot of difrential diagnosis with other diseases therefore texture analysis can provide second opinion for the radiologist to diagnose brain pathologies with some confident as well as it will draw his attention to the area of interest .

1.3. Objectives:

General objective:

The general objective of this study is to is to characterizethe MS in MR images using Texture analysis in order to reduce the miss detection rate.

Specific objective:

- To extract texture feature from MR images using first order statistics.
- To classify the extracted feature into four classes including MS plaques using K-means through Euclidian distance.
- To generate a classification map from the classified features.
- To apply linear discriminate analysis to generate model for linear classification on FLAIR and T2 Imaging .
- To calculate the sensitivity, specificity and accuracy .
- To use to discriminate analysis in difrentiation btween MS and other disease apear like it on the MR image (SVD) .

1.4. Significant of the study:

This study will highlight the application of image analysis using image processing technique in characterizing brain pathologies on MR images , and hence it will facilitate quantitative approach in brain defect.

1.5. Hypothesis of the study:

The hypothesis is that by examining the nature of gray-level transitions in medical images, we can extract a subset of textural features, that will best characterize the pathology or disease process of interest (eg: MS).

1.6. Overview of the study

This study will falls into five chapters. Chapter one is an introduction as well as statement of the problem and study objective and significance of the study. While Chapter two will include literature review ,and anatomical background and previous studies. Chapter three deals with the methodology, where it provides an outline of material and methods used to acquire the data in this study as well as the method of analysis approach. While the results were present in chapter four, and finally Chapter five include discussion of the results, conclusion and recommendation followed by references and appendices.
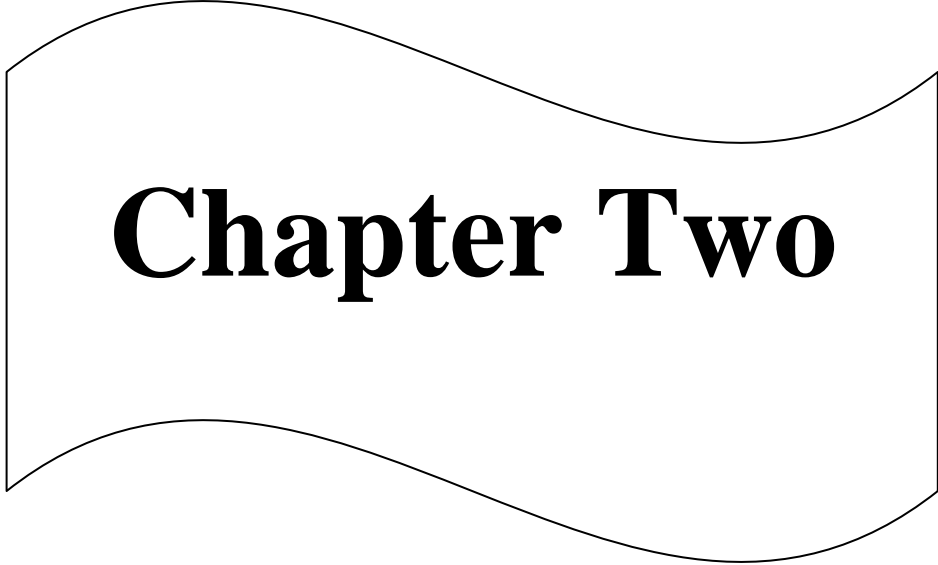
Chapter Two

Chapter Two

Literature Review

2.1 Anatomy:

The CNS has two main divisions:

The brain, which occupies the cavity of the cranium.

The solid spinal cord, which extends inferiorly from the brain and is protected by the bony vertebral column. The solid spinal cord terminates at the lower border of first lumber vertebra, with a tapered area called the conus medullaris Nerve root extensions of the spinal cord continue down to the first coccyx segment. The subarachnoid space continues down to the second segment of the sacrum. (Bontrager, 2014)

2.1.1 Neuron:

Neurons, or nerve cells, are the specialized cells of the nervous system that conduct electrical impulses. Each neuron is composed of an axon, a cell body, and one or more dendrites.

Dendrites are processes that conduct impulses toward the neuron cell body. An axon is a process that leads away from the cell body. The dendrites and cell bodies make up the gray matter of the brain and spinal cord, and the large myelinated axons make up the white matter. (Bontrager, 2014)
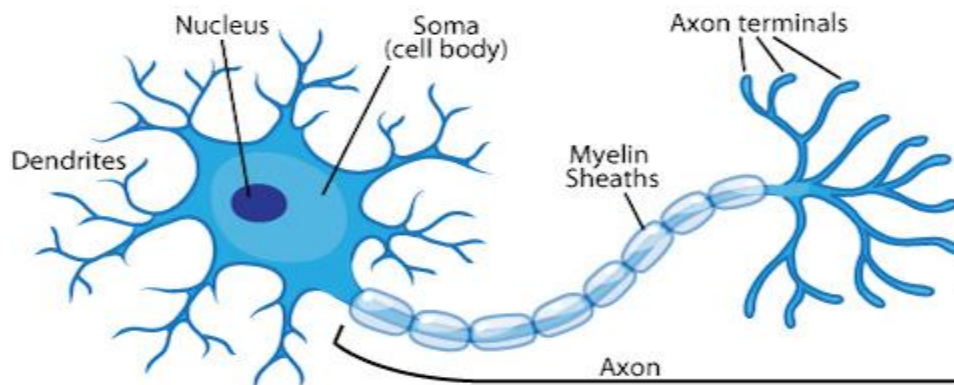
Fig (2-1): the Neuron

2.1.2 Brain and Spinal Cord Coverings—Meninges

Both the brain and the spinal cord are enclosed by three protective coverings or membranes termed meninges. Starting externally, these are :

1) Dura mater The outermost membrane is the dura mater, which means "hard" or "tough mother." It's strong, fibrous brain covering.

2) Pia mater The innermost of these membranes is the pia mater, literally meaning "tender mother." This membrane is very thin and highly vascular and lies next to the brain and spinal cord. It encloses the entire surface of the brain, dipping into each of the fissures and sulci.

3) Arachnoid Between the pia mater and the dura mater is a delicate avascular membrane called the arachnoid mater. (Bontrager, 2014)
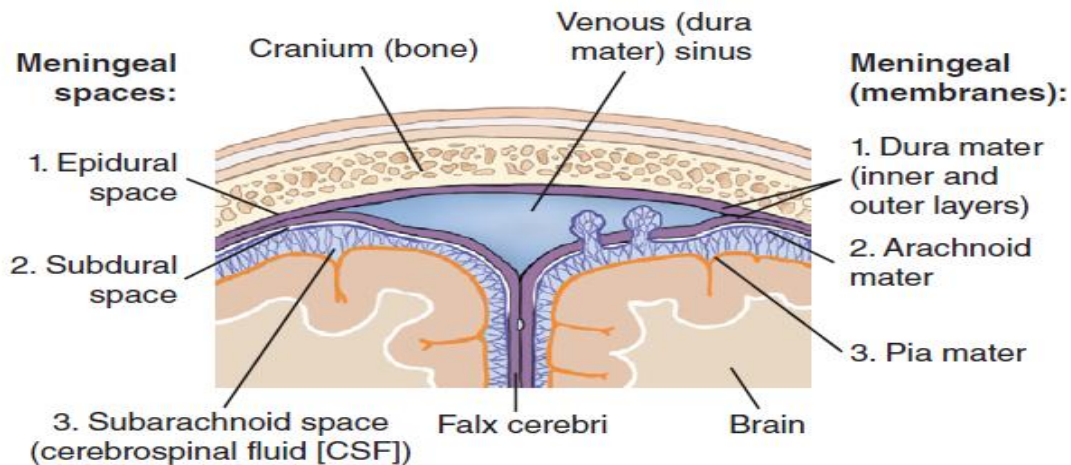
Fig (2-2): the Meninges (Bontrager 2014)

2.1.3 Three Divisions of Brain

The brain can be divided into three general areas: (1) forebrain, (2) midbrain, and (3) hindbrain. These three divisions of the brain are divided further into specific areas and structures. (Bontrager, 2014)
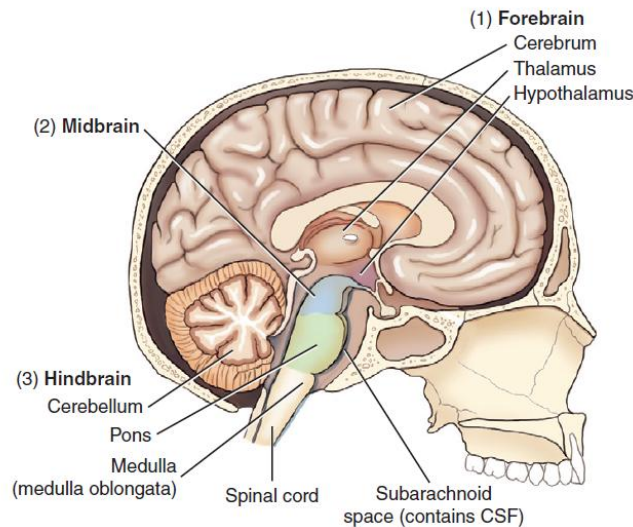
Fig (2-3): shown the three divisions of the brain (Bontrager, 2014)

2.1.3.1. Forebrain:

It consists of three parts the first part of the forebrain is the large cerebrum, the second part is the thalamus and the third and final division of the forebrain is the hypothalamus. (Bontrager, 2014)

2.1.3.1.1 Cerebrum:

The relative sizes of various structures, including the five lobes of the cerebrum. The surface layer of the entire cerebrum, about 2 to 4 mm in thickness, directly under the bony skull cap is called the cerebral cortex. The total cerebrum occupies most of the cranial cavity. (Bontrager, 2014)

Five Lobes of Each Cerebral Hemisphere Each side of the cerebrum is termed a **cerebral hemisphere** and is divided into five lobes. The four lobes lie beneath the cranial bones of the same name. The frontal lobe lies under the frontal bone, with the parietal lobe under the parietal bone. Similarly, the occipital lobe and the temporal lobe lie under their respective cranial bones. The fifth lobe, termed the insula, or central lobe, is more centrally located. (Bontrager, 2014)

Cerebral Hemispheres;

The cerebrum is partially separated by a deep longitudinal fissure in the mid-sagittal plane. This fissure divides the cerebrum into right and left cerebral hemispheres. Parts of the frontal, parietal, and occipital lobes .

The surface of each cerebral hemisphere is marked by numerous grooves and convolutions, which are formed during the rapid embryonic growth of this portion of the brain. Each convolution or raised area is termed a **gyrus**. A **sulcus** is a shallow groove, and the central sulcus, which divides the frontal and parietal lobes of the cerebrum, is a landmark used to identify specific sensory areas of the cortex. (Bontrager, 2014)

A deeper groove is called a fissure, such as the deep longitudinal fissure that separates the two hemispheres.

The corpus callosum, located deep within the longitudinal fissure and not visible on this drawing, consists of an arched mass of transverse fibers (white matter) connecting the two cerebral hemispheres. (Bontrager, 2014)

(A)   (B)
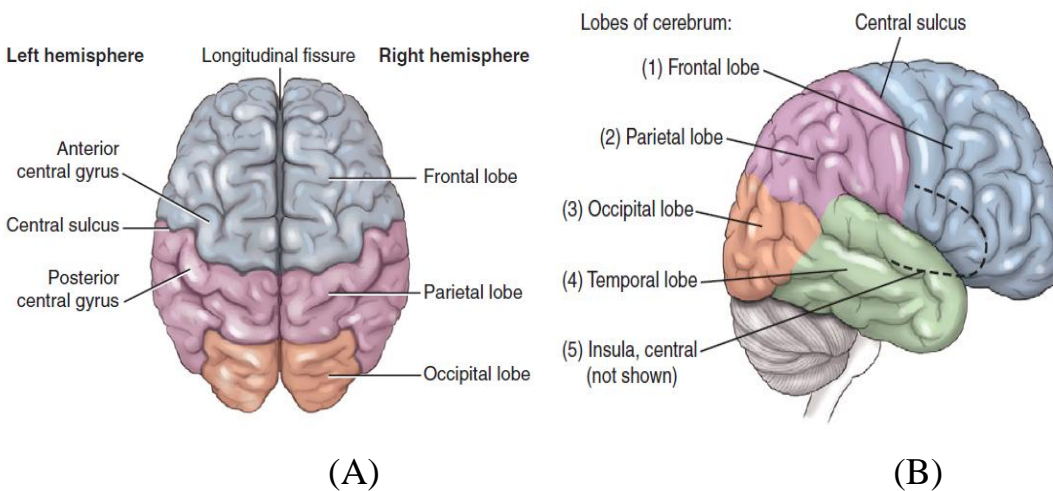
Fig (2-4): lobes of the brain (A) superior view &(B) lateral view (Bontrager, 2014)

2.1.3.1.2Cerebral Ventricles:

The ventricular system of the brain is connected to the subarachnoid space. There are four cavities in the ventricular system. These four cavities are filled with CSF and inter connect through small tubes.

The right and left lateral ventricles are located in the right and left cerebral hemispheres. (Bontrager, 2014)

The third ventricle is a single ventricle that is located centrally and inferior to the lateral ventricles. (Bontrager, 2014)

The fourth ventricle is also a single ventricle located centrally, just inferior to the third ventricle. (Bontrager, 2014)

CSF is formed in the lateral ventricles in capillary beds called choroid plexus, which filter the blood to form CSF. (Bontrager, 2014)

2.1.3.2 Midbrain and Hindbrain

The midbrain is seen as a short, constricted portion of the upper brainstem that connects the forebrain to the hindbrain. The hindbrain consists of the cerebellum, pons, and medulla. The cerebellum is the largest portion of the hindbrain and the second largest portion of the entire brain. (Bontrager, 2014)

2.1.4 Gray Matter and White Matter

The CNS can be divided by appearance into white matter and gray matter. White matter in the brain and spinal cord is composed of tracts, which consist of bundles of myelinated axons. Myelinated axons are axons wrapped in a myelin sheath, a fatty substance having a creamy white color. The white matter comprises mostly axons. (Bontrager, 2014)

Gray Matter The gray matter comprises the thin outer layer of the folds of the cerebral cortex and is composed of dendrites and cell bodies. Other gray matter of the brain includes more central brain structures, such as the cerebral nuclei or basal ganglia, located deep within the cerebral hemispheres, and the groups of nuclei that make up the thalamus. whereas the brain tissue under the cortex is white matter. This underlying mass of white substance is termed the centrum semiovale which are fibers that connect the gray matter of the cerebral cortex with the deep, more caudal parts of the midbrain and spinal cord. (Bontrager, 2014)

The second major white matter structure is the corpus callosum a band of fibers that connect the right and left cerebral hemispheres deep within the longitudinal fissure. (Bontrager, 2014)
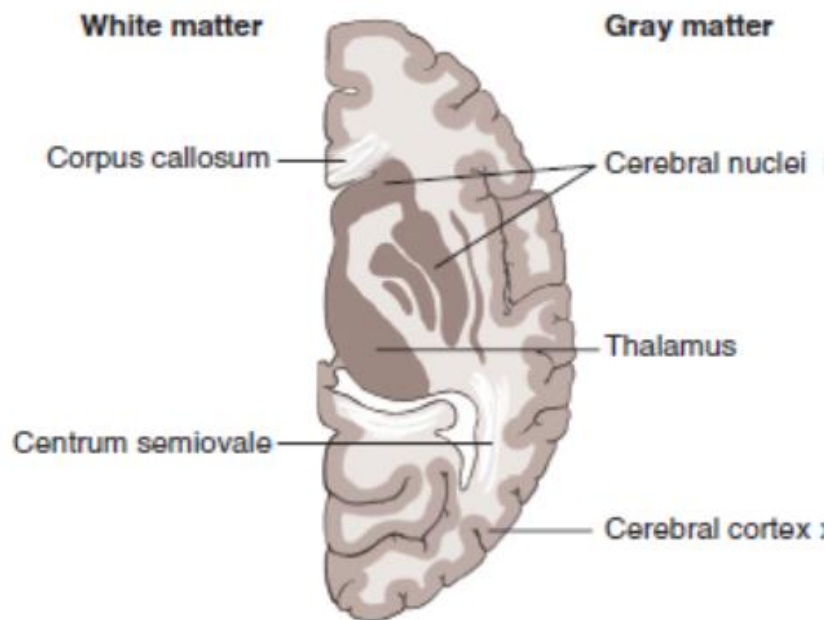
Fig (2-5): A section of brain tissue through the cerebral hemispheres (Bontrager, 2014)

2.1.5 Cerebral Nuclei (Basal Ganglia)

The cerebral nuclei, or basal ganglia, are paired collections of gray matter deep within each cerebral hemisphere. There are four specific areas or groupings of

9

these cerebral nuclei: the (1) caudate nucleus; (2) lentiform nucleus, comprising putamen and globuspallidus; (3) claustrum and (4) amygdaloid nucleus or body. (Bontrager, 2014)

2.1.6 Arterial Supply and venous daring:

2.1.6.1 Arterial Supply :

The brain receives arterial blood from two main pair of vessels and their branches, the internal carotid arteries and the vertebral arteries. Many normal variations of the arterial blood supply exist. (Kelley, 2007)

The Internal Carotid Arteries supply the frontal, parietal, and temporal lobes of the brain and orbital structures. These arteries arise from the bifurcation of the carotid arteries in the neck. The internal carotid artery then turns forward within the cavernous sinus, then up and backward through the dura mater, forming an S shape (carotid siphon) before it reaches the base of the brain . As the internal carotid artery exits the cavernous sinus, it branches into the ophthalmk artery just inferior to the anterior clinoid process. The internal carotid artery then runs lateral to the optic chiasm and branches into the anterior cerebral artery and the larger middle cerebral artery. The anterior cerebral artery and its branches supply the anterior frontal lobe and the medial aspect of the parietal lobe . The middle cerebral artery is by far the largest of the cerebral arteries and is considered a direct continuation of the internal carotid artery. The middle cerebral artery gives off many branches, as it supplies much of the lateral surface of the cerebrum, insula, and anterior and lateral aspects of temporal lobe; nearly all the basal ganglia; and the posterior and anterior internal capsule.(Kelley, 2007)

Vertebral Arteries The vertebral arteries begin in The neck at the subclavian artery and ascend vertically through the transverse foramina of the cervical spine. The vertebral arteries curve around the atlanto-occipital joints to enter the cranium

through the foramen magnum . The two vertebral arteries unite ventral to the pons, to form the basilar artery . The vertebral and basilar arteries give rise to several pairs of smaller arteries that supply the cerebellum, pons, and inferior and medial surfaces of the temporal and occipital lobes. The four major pairs of arteries are listed in order from inferior to superior: posterior inferior cerebellar, anterior inferior cerebellar, superior cerebellar , and posterior cerebral . The posterior cerebral arteries can be divided into three major segments: precommunicating or peduncular (Pl), ambient (P2), and quadrigeminal (P3) . The posterior communicating artery forms a connection between the posterior cerebral artery and the internal carotid artery .

(Kelley, 2007)

Circle Of Willis : The cerebral arterial circle, or circle of Willis, is a critically important anastomosis among the four major arteries (two vertebral and two internal carotid) feeding the brain. The circle of Willis is formed by the anterior and posterior cerebral, anterior and posterior communicating, and the internal carotid arteries. The circle is located mainly in the suprasellar cistern at the base of the brain. Many normal variations of this circle may occur in individuals. The circle of Willis functions as a means of collateral blood flow from one cerebral hemisphere to another in the event of blockage .(Kelley, 2007)
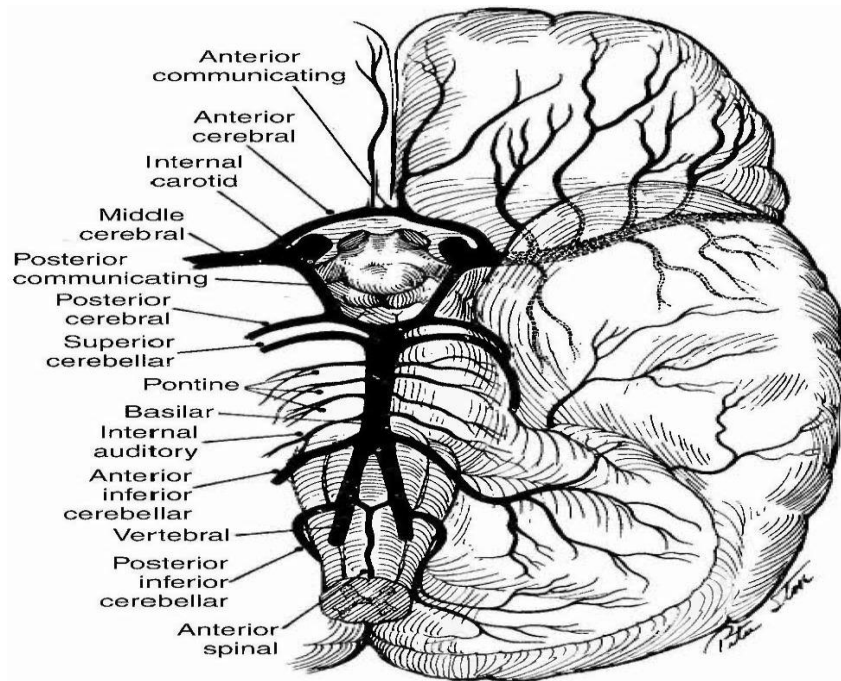
Fig (2-6): Circle Of Willis.(Kelley, 2007)

2.1.6.2 Venous Drainage:

The venous system of the brain and its coverings is composed primarily of the dural sinuses, superficial cortical veins, and deep veins of the cerebrum. Dural Sinuses The dural sinuses are very large veins located within the dura mater of the brain. All the veins of the head drain into the dural sinuses and ultimately into the internal jugular veins of the neck. The major dural sinuses include superior and inferior sagittal, straight, transverse, sigmoid, cavernous, and petrosal . The superior sagittal sinus lies in the medial plane between the falx cerebri and the calvaria. It begins at the crista galli, runs the entire length of the falx cerebri, and ends at the internal occipital protuberance of the occipital bone . The inferior sagittal sinus, which is much smaller than the superior sagittal sinus, runs posteriorly just under the free edge of the falx cerebri The nferior sagittal sinusconverges with the great cerebral vein (vein of Galen) to form the straight sinus. The straight sinus extends along the length of the junction of the falx cerebri

and the tentorium cerebelli . The junction of the superior sagittal, transverse, and straight sinuses creates the large confluence of the sinuses .The transverse sinuses extend from the confluence between the attachment of the tentorium and the calvaria. As the transverse sinuses pass through the tentorium cerebelli, they become the sigmoid sinuses. The S-shaped sigmoid sinuses continue in the posterior cranial fossa to join the jugular bulbs of the internal jugular veins .(Kelley, 2007)

The cavernous sinuses, located on each side of the sella and body of the sphenoid bone. Each cavernous sinus receives blood from the superior and inferior ophthalmic veins and communicates with the transverse sinuses by way of the petrosal sinuses .(Kelley, 2007)
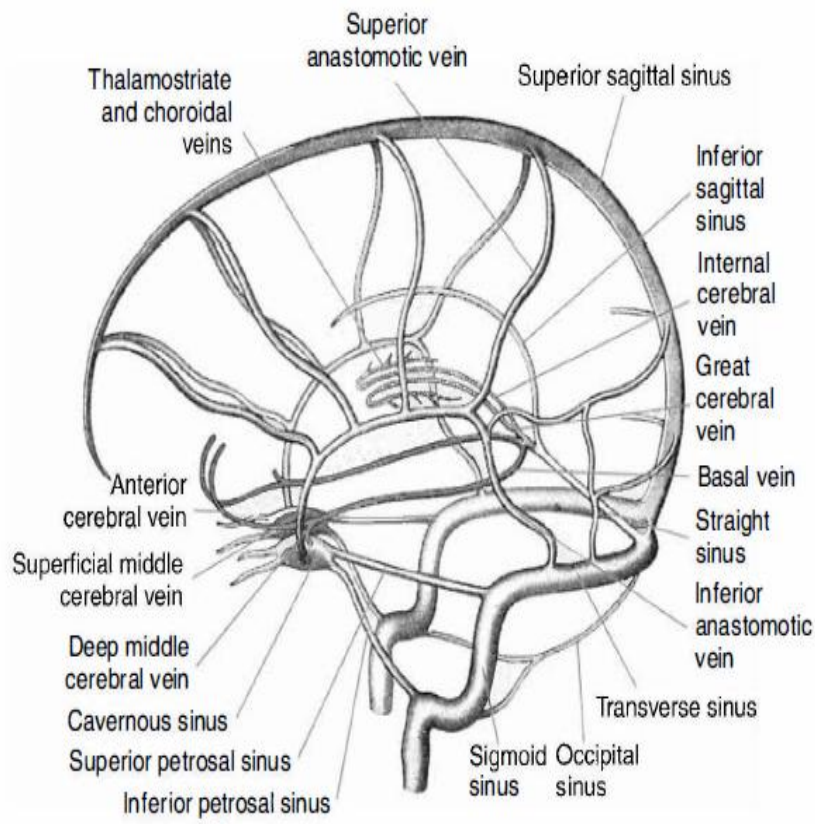
Fig (2-7): Venous Drainage.(Kelley2007)

2.2 Physiology of the nervous system:

The divisions of the nervous system can be classified by location or by the type of tissue supplied by the nerve cells in the division. The **central nervous system (CNS)** consists of the brain and spinal cord. The remaining neural structures, including 12 pairs of cranial nerves, 31 pairs of spinal nerves, autonomic nerves, and ganglia, make up the **peripheral nervous system** which consists of afferent and efferent neurons. Afferent (sensory) neurons conduct impulses from peripheral receptors to the CNS. (Eisenberg, 2012)

Efferent (motor) neurons conduct impulses away from the CNS to the peripheral effectors. The **somatic nervous system** supplies the striated skeletal muscles, whereas the **autonomic nervous system** supplies smooth muscle, cardiac muscle, and glandular epithelial tissue. (Eisenberg ,2012)

The basic unit of the nervous system is the **neuron,** or nerve cell. A neuron consists of a cell body and two types of long, threadlike extensions. A single axon leads from the nerve cell body, and one or more dendrites lead toward it. Axons are insulated by a fatty covering called the **myelin sheath,** which increases the rate of transmission of nervous impulses. (Eisenberg, 2012)

In involuntary reactions the impulse conduction route to and from the CNS is termed a **reflex arc.** Voluntary actions are commonly a reaction due to stimulation of a combination of sensors. The basic reflex arc consists of an afferent, or sensory, neuron, which conducts impulses to the CNS from the periphery; and an efferent, or motor, neuron, which conducts impulses from the CNS to peripheral effectors (muscles or glandular tissue). (Eisenberg, 2012)

Impulses pass from one neuron to another at a junction called the **synapse.** Transmission at the synapse is a chemical reaction in which the termini of the axon release a neurotransmitter substance that produces an electrical impulse in the dendrites of the next axon. Once the neurotransmitter has accomplished its task, its

activity rapidly terminates so that subsequent impulses pass along this same route.(Eisenberg, 2012).

The cerebral cortex is responsible for receiving sensory information from all parts of the body, and for triggering impulses that govern all motor activity. Just posterior to the central sulcus, the cerebral cortex has specialized areas to receive and precisely localize sensory information from the peripheral nervous system. Visual impulses are transmitted to the **posterior portion** of the brain; olfactory (smell) and auditory impulses are received in the **lateral portions**. The primary motor cortex is just anterior to the central sulcus. Because efferent motor fibers cross over from one side of the body to the other at the level of the medulla and spinal cord, stimulation on one side of the cerebral cortex causes contraction of muscles on the opposite side of the body. (Eisenberg, 2012)

The premotor cortex, which lies anterior to the primary motor cortex, controls movements of muscles by stimulating groups of muscles that work together. This region also contains the portion of the brain responsible for speech, which is usually on the left side in right-handed people. In addition, the cerebral cortex is the site of all higher functions, including memory and creative thought. The two cerebral hemispheres are connected by a mass of white matter called the **corpus callosum.** These extensive bundles of nerve fibers lie in the midline just above the roofs of the lateral ventricles. (Eisenberg, 2012)

2.3. Pathology:

2.3.1. Infections of the central nervous system:

The incidence of infectious diseases of the CNS has decreased with the widespread availability of antibiotics. Nevertheless, bacterial, fungal, viral, and protozoal

organisms can infect the brain parenchyma, meningeal linings, and bones of the skull.(Eisenberg, 2012)

Meningitis:

Meningitis is an acute inflammation of the pia mater and arachnoid, two of the membranes covering the brain and spinal cord. (Eisenberg, 2012)

Brain Abscess:

Brain abscesses are usually a result of chronic infections of the middle ear, paranasal sinuses, or mastoid air cells, or of systemic infections (pneumonia, bacterial endocarditis, osteomyelitis). (Eisenberg, 2012)

2.3.2. Tumors of the central nervous system:

Intracranial neoplasms manifest clinically as seizure disorders or gradual neurologic deficits (difficulty thinking, slow comprehension, weakness, headache). About 50% of CNS tumors are primary lesions, and the others represent metastases. (Eisenberg, 2012)

Glioma:

Gliomas, the most common primary malignant brain tumors, consist of glial cells (supporting connective tissues in the CNS) that still have the ability to multiply. They spread by direct extension and can cross from one cerebral hemisphere to the other through connecting white matter tracts, such as the corpus callosum. (Eisenberg, 2012)

Meningioma:

Meningiomas are benign tumors that arise from arachnoid lining cells and are attached to the dura. The most common sites of meningioma are the convexity of the calvaria, the olfactory groove, the tuberculumsellae, the parasagittal region, the sylvian fissure, the cerebellopontine angle, and the spinal canal. (Eisenberg, 2012)

Acoustic Neuroma:

Acoustic neuromas are slowly growing benign tumors that may occur as solitary lesions or as part of the syndrome of neurofibromatosis. Such a tumor arises from Schwann cells in the vestibular portion of the auditory(eighth cranial) nerve. (Eisenberg, 2012)

Metastatic Carcinoma:

Carcinomas usually reach the brain by hematogenous spread. Infrequently, epithelial malignancies of the nasopharynx can spread into the cranial cavity through neural foramina or by direct invasion through bone., colon carcinomas, and testicular and kidney tumors also cause brain metastases(Eisenberg, 2012)

2.3.3. Traumatic Processes of the Brain:

Epidural Hematoma:

Epidural hematomas are caused by acute arterial bleeding and most commonly form over the parietotemporal convexity. Acute arterial bleeding is usually caused by laceration of the medial meningeal artery. (Eisenberg, 2012)

Subdural Hematoma:

Subdural hematomas reflect venous bleeding, most commonly from ruptured veins between the dura and meninges. (Eisenberg, 2012)

Intracerebral Hematoma:

Traumatic hemorrhage into the brain parenchyma can result from shearing forces to intraparenchymal arteries, which tend to occur at the junction of the gray and white matter. Injury to the intima of intracranial vessels can cause the development of traumatic aneurysms, whichcan rupture. (Eisenberg, 2012)

2.3.4. Vascular disease of the central nervous system:

The term **cerebrovascular disease** refers to any process that is caused by an abnormality of the blood vessels or blood supply to the brain. Pathologic processes causing cerebrovascular disease include abnormalities of the vessel wall, occlusion by thrombus or emboli, rupture of blood vessels with subsequent hemorrhage, and decreased cerebral blood flow caused by lowered blood pressure or narrowed lumen caliber. Cerebrovascular diseases include arteriosclerosis, hypertensive hemorrhage, arteritis, aneurysms, and arteriovenous malformations . (Eisenberg, 2012)

2.3.5. Multiple sclerosis:

Multiple sclerosis (MS) is an inflammatory, autoimmune, demyelinating disease of the central nervous system. It generally strikes at an early age, most often the early adult years. Its most frequent symptoms include numbness, impaired vision, loss of balance, weakness, bladder dysfunction, and psychological changes. Fatigue is an early symptom in MS, often the earliest. The disease can wax and wane for up to 30 years, but in perhaps half of all cases it steadily progresses to severe disability and premature death.(Parris, 2001)

MS owes its name to the presence of multiple sclerotic (hardened) lesions in the brain and spinal cord – multiple scars. The optic tract also is often involved. This disease has major autoimmune character, with T-cells and other immune effector populations entering the brain and attacking the nerve cells, stripping away their myelin insulation and sometimes destroying their axons and entire remaining structures. Principal patterns of demyelination and axonal degeneration are schematized in Fig (2-8).

(Parris, 2001)

MS is the most common cause of neurologic disability in young adults. The lesions of demyelination are histo-pathologically characteristic of the disease. Brain examination by MRI can accurately detect these "white matter plaques." MRI

correlates well with the classic histopathology of the lesions, and is progressively a more sensitive tool for detecting the characteristic lesions of MS in situ, as compared to conventional functional evaluation. (Parris, 2001)
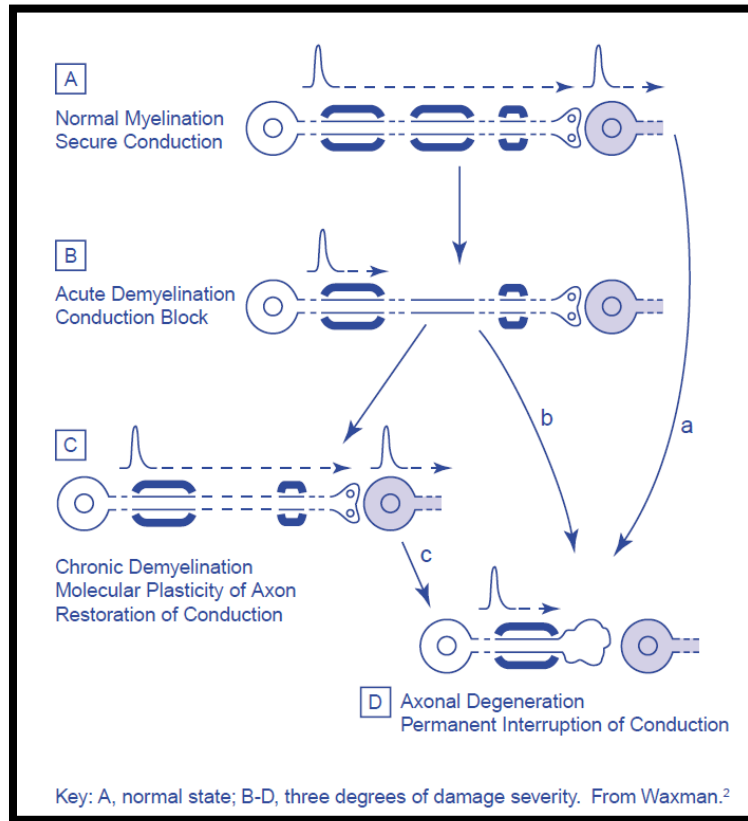
Fig (2-8): Demyelination and Axonal Degeneration in Multiple Sclerosis (Parris, 2001)

Currently approved drug therapies for MS are highly toxic; the immune-suppress antscortisone, prednisone, methotrexate, and cytoxan are still mainstays of conventional MS management. In 1993, interferon -1b was approved in the United States as attack prevention therapy, but this drug itself is burdened with frequent and severe adverse effects. The limitations of the conventional drug therapies for MS make imperative the development of a less toxic, integrative strategy for its management.

(Parris, 2001)

2.3.6. Degenerative diseases:

Alzheimer's Disease:

Alzheimer's disease (presenile dementia) is a diffuse form of progressive cerebral atrophy that develops at an earlier age than the senile period. (Eisenberg, 2012)

Cerebellar Atrophy:

Isolated atrophy of the cerebellum may represent an inherited disorder, a degenerative disease, or the toxic effect of prolonged use of such drugs as alcohol and phenytoin (Dilantin) (Eisenberg, 2012)

2.4. MRI physics :

Magnetic resonance imaging it is the function of proton spin density and relaxation time.

To make MR image we need:

Primary magnet.

RF trans-receiver coil.

Gradient coil.

In addition to the ordinary computer input devices including the processing unit that use to reconstruct the MRI image and display it on the screen or store it in a disk.(Evert, 2004)

2.4.1.Physical principal

MRI image depend on the presence of protons which is electrically charged and it rotates around its axis (spinning),this rotation generate a magnetic field around

each proton (In our body these tiny bar magnets (protons) are ordered in such a way that the magnetic forces equalize) . (Evert, 2004)

The proton in the hydrogen (has 1 proton and 1 electron) were used to generate MRI image because first off all we have a lot of them in the human body and secondly the gyro magnetic ratio for Hydrogen is the largest; 42.57 MHz/Tesla. (Evert, 2004)

When put the hydrogen protons under the magnet they align with the magnetic field. This is happened in two ways, parallel and anti-parallel and process or "wobble" due to the magnetic momentum of the atom. (Evert, 2004)

A   B
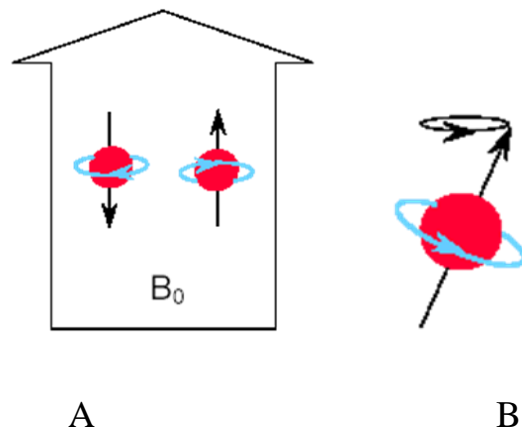
Fig (2-9): protons under the magnet they align with the magnetic field (A) and precess or "wobble"(B) (B_0 is the indication for the magnetic field of the MRI scanner). (Evert, 2004)

This protons precess at the Larmor frequency which can be calculated from the following equation:

$$\omega_0 = \gamma \, B_0$$

Where: ω_0 = Precessional or Larmor frequency. (MHz)

                 γ = Gyro Magnetic Ratio. (MHz/T)

                 B_0 = Magnetic field strength. (T)

The Larmor frequency is needed to calculate the operating frequency of the MRI system, (Evert, 2004)

When protons align with the magnetic field more protons aligned parallel or low energy state than there are anti-parallel or high energy state and the number of excess protons is proportional with B0. (Evert, 2004)

At the end there is a net magnetization (the sum of all tiny magnetic fields of each proton) pointing in the same direction as the system's magnetic field. (Evert, 2004)

2.4.2.The MRI image acquisition can be summarized into:

2.4.2.1 Excitation

Before the system starts to acquire the data it will perform a quick measurement (also called pre-scan) to determine at which frequency the protons are spinning (the Larmor frequency). This centre frequency is important because this is the frequency the system uses for the excitation step in which the proton were excited by sending and RF frequency.

(Evert, 2004)

This is where the Resonance comes from in the name Magnetic Resonance Imaging.

protons that spin with the same frequency as the RF pulse will respond to that RF pulse therefore the net magnetization will be "flipped" 90º.(It is possible to flip the net magnetization any degree in the range from 1º to 180º). (Evert, 2004)

This process is called excitation. (Evert, 2004)

2.4.2.2 Relaxation

When the net magnetization was rotated 90º into the X-Y plane this happened because the protons absorbed energy from the RF pulse this is a situation that the protons do not like (they prefer to align with the main magnetic field) when the RF of now something happens that is referred to as Relaxation. (Evert, 2004)

The relaxation process can be divided into two parts: T1 and T2 relaxation. (Evert, 2004)

2.4.2.2.1 T1 Relaxation:

T1 is defined as the time it takes for the longitudinal magnetization (Mz) to reach 63 % of the original magnetization. Each tissue will release energy (relax) at a different rate and that's why MRI has such good contrast resolution. (Evert, 2004)

The protons want to go back to their original situation they do so by releasing the absorbed energy in the shape of (very little) warmth and RF waves in principle the reverse of excitation takes place(The net magnetization rotates back to align itself with the Z-axis). (Evert, 2004)

T1 Relaxation Curves

T1 relaxation happens to the protons in the volume that experienced the 90º-excitation pulse but not all the protons are bound in their molecules in the same way. One ^{1}H atom may be bound loosely , will release their energy much quicker

to their surroundings than protons, which are bound tightly . The rate at which they release their energy is therefore different. (Evert, 2004)

2.4.2.2.2 T2 Relaxation

T2 is defined as the time it takes for the spins to de-phase to 37% of the original value. (Evert, 2004)

T1 and T2 relaxation are two independent processes. The only thing they have in common is that both processes happen simultaneously.T1 relaxation describes what happens in the Z direction, while T2 relaxation describes what happens in the X-Y plane. (Evert, 2004)

T2 Relaxation Curves

Just like T1 relaxation, T2 relaxation does not happen at once. Again, it depends on how the Hydrogen proton is bound in its molecule and that again is different for each tissue. (Evert, 2004)
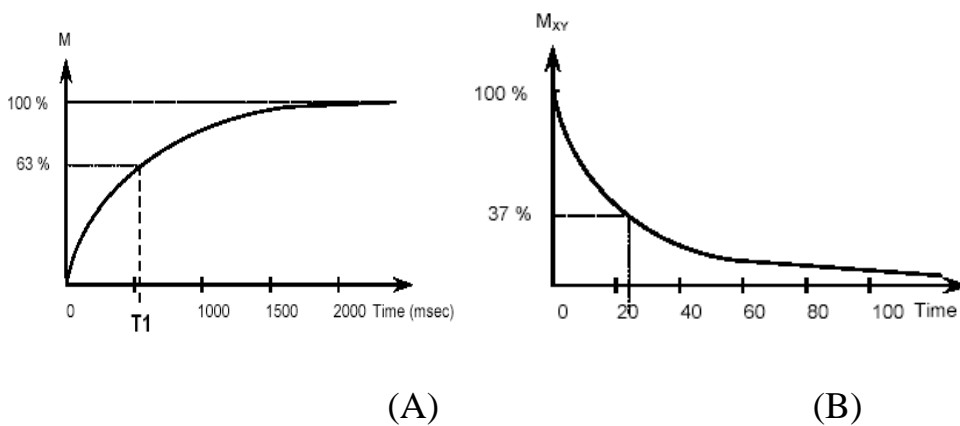

(A)   (B)

Fig (2-10): T1 (A) and T2 (B) relaxation curves. (Evert, 2004)

Right after the 90° RF-pulse all the magnetization is "flipped" into the XY plane the net magnetization changes name and is now called M_{XY}. At time = 0 all spins

are in-phase, but immediately start to de-phase. T2 relaxation is also a time constant. (Evert, 2004)

2.4.2.3 Acquisition

During the relaxation processes the spins shed their excess energy, which they acquired from the 90° RF pulse, in the shape of radio frequency waves. In order to produce an image we need to pick up these waves before they disappear into the space. (Evert, 2004)

This can be done with a Receive coil

If we assume we have a 100% homogeneous magnetic field then all the protons in the body would spin at the Larmor frequency. This also means that all protons would return signal. (Evert, 2004)

How do we know the location of coming signal?

The solution to this problem can be found in the properties of an RF-wave, which are: phase, frequency and amplitude.

First we will divide the body up into volume elements, also known as: voxels. Then we are going to code the voxels such that the protons, within that voxel, will emit an RF wave with a known phase and frequency. The amplitude of the signal depends on the amount of protons in the voxel this could be done using the Gradient Coils. (Evert, 2004)

Gradient coil

Gradient coils are a set of wires in the magnet, which enable us to create additional magnetic fields, which are, in a way, superimposed on the main magnetic field B0. (Evert, 2004)

2.4.2.3.1 Signal Coding

2.4.2.3.1.1 Slice Encoding Gradient

If the Z- gradient is switched on. This will generate an additional magnetic field in the Z direction, which is superimposed on B0. The indication +Gz means there is a slightly stronger B0 field in the head as there is in the iso-centre of the magnet. A stronger B0 field means a higher Larmor frequency. Along the entire slope of the gradient there is a different B0 field and consequently the protons spin at slightly different frequencies. (Evert, 2004)

Within the slice there are still a lot of protons and we still don't know from where the signal is coming from within the slice whether it comes from anterior, posterior, left or right, further encoding is therefore required . (Evert, 2004)

2.4.2.3.1.2 Phase Encoding Gradient

In order to code the protons further the Gy gradient is switched on very briefly. During the time the gradient is switched on an additional gradient magnetic field is created in the anterior-posterior direction. The effect is that the anterior protons will spin slightly faster than the posterior protons. (Evert, 2004)

When the Gy gradient is switched off, each proton within the slice spins with the same frequency BUT each has a different phase.

We can determine two things:

The signal comes from which slice (Slice Encoding)

The signal contains a number of RF waves, which have the same frequency, but have different phases.

It is possible to tell whether the signal comes from anterior or from posterior. (Phase Encoding) all we need to do now is to do one more encoding to determine whether the signal comes from the left, the centre or the right side of the head. (Evert, 2004)

2.4.2.3.1.3 Frequency Encoding Gradient

To encode in the left – right direction the third, and last, gradient (Gx) is switched on. This will create an additional gradient magnetic field in the left – right direction. (Evert, 2004)

The protons on the left hand side spin with a lower frequency than the ones on the right. They will accumulate an additional phase shift because of the different frequency, but – and this is utterly important - the already acquired phase difference, generated by the Phase Encoding gradient in the previous step, will remain. (Evert, 2004)
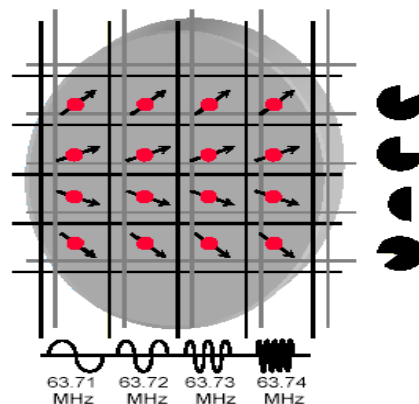

Fig (2-11): action of phase & frequency Encoding Gradients.(Evert, 2004)

Therefore We can pinpoint the exact origin of the signals, which are received by the coil using the frequency and the phase. (Evert, 2004)

As a result small volumes (voxels) have been created. Each voxel has a unique combination of frequency and phase. The amount of protons in each voxel determines how strong (amplitude) the RF-wave . The signal received contains a complex mix of frequencies, phases and amplitudes each from a different location (voxel) within the slice. (Evert, 2004)

2.5 MRI Technique

2.5.1 Equipment:

 Head coil (quadrature or multi-coil array).

Immobilization pads and straps.

Ear plugs.

High-performance gradients for EPI, diffusion and perfusion imaging.

(Westbrook, 2008)

2.5.2 Patient positioning:

The patient lies supine on the examination couch with their head within the head coil. The head is adjusted so that the inter-pupillary line is parallel to the couch and the head is straight. The patient is positioned so that the longitudinal alignment light lies in the midline, and the horizontal alignment light passes through the nasion. Straps and foam pads are used for immobilization.(Westbrook, 2008)

2.5.3 Suggested protocol

Sagittal SE/FSE/incoherent (spoiled) GRE T1

Medium slices/gap are prescribed on each side of the longitudinal alignment light from one temporal lobe to the other. The area from the foramen magnum to the top of the head is included in the image. (Westbrook, 2008)

Axial/oblique SE/FSE PD/T2

Medium slices/gap are prescribed from the foramen magnum to the superior surface of the brain. Slices may be angled so that they are parallel to the anterior–

posterior commissure axis. This enables precise localization of lesions from reference to anatomy atlases (Figures 8.3 and 8.4). Many sites have replaced the PD sequence with FLAIR .

SS-FSE or SS-EPI may be a necessary alternative for a rapid examination in uncooperative patients. (Westbrook, 2008)
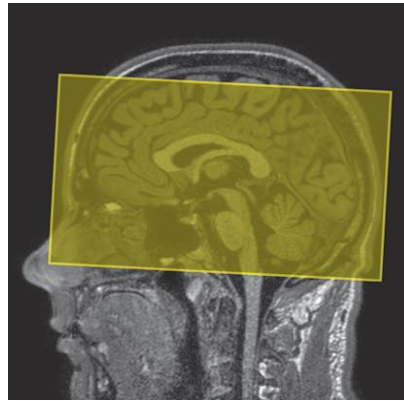

Fig (2-12): Sagittal SE T1 weighted midline slice of the brain showing slice prescription boundaries and orientation for axial/oblique imaging.

(Westbrook, 2008)

Coronal SE/FSE PD/T2

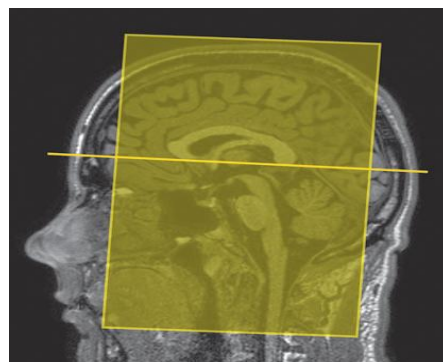As for Axial PD/T2, except prescribe slices from the cerebellum to the frontal lobe (Fig (2-16)). (Westbrook, 2008)

Fig (2-13): Sagittal SE T1 weighted image showing slice prescription boundaries and orientation for coronal imaging. (Westbrook, 2008)

2.5.4 Additional sequences

Axial/oblique FLAIR/EPI (Fig(2-17))

Slice prescription as for Axial/oblique T2. This sequence provides a rapid acquisition with suppression of CSF signal. It may be useful when examining periventricular or cord lesions such as MS plaques.

(Westbrook, 2008)
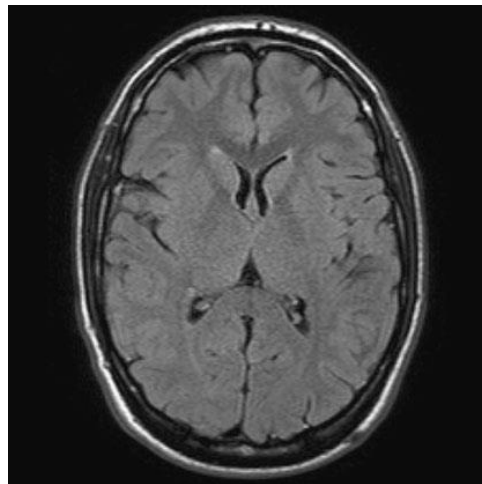
Fig (2-14): Axial/oblique FLAIR image of the brain. Periventricular abnormalities will have a high signal intensity in contrast to the low signal of CSF which has been nulled using a long TI.(Westbrook, 2008)

2.6 Deferential diagnoses of MS

MRI is far superior to CT and typically demonstrates ovoid high T2W signal lesions within the corpus callosum and periventricular white matter that typically lie perpendicular to the ventricular margin. Other characteristic sites include the optic radiation, brainstem (dorsal), cerebellar peduncles and optic nerves. Abnormalities in the cerebral cortex, deep grey nuclei and 'peripheral' white matter

are less common, but are by no means rare. Acute lesions are usually ill-defined and may display surrounding oedema. The latter contributes to the 'target' appearance that is sometimes seen with acute plaques. Solid and 'ring-like' contrast uptake is a feature of acute demyelination, regardless of the cause. Large acute lesions may be mistaken for tumors if there is considerable mass effect. As lesions age they shrink, become more circumscribed and fail to enhance with contrast medium. Sagittal T2W, proton density and FLAIR sequences are recommended for routine diagnostic purposes. (Chapman, 2003)

Differential Diagnosis:

2.6.1 Normal

A. **Age-related white matter lesions** — small peripheral white matter lesions are commonly seen in the normal ageing brain. Periventricular lesions are best seen on FLAIR MRI and may present as a thin uniform rim, frontal 'caps' or more patchy areas of signal change. The loose term small vessel ischaemia' is a convenient, but inaccurate, description of most age-related white matter change. (Chapman, 2003)

2.6.2 Vascular

A. **'Small vessel disease'** — premature cerebrovascular disease in hypertensive and diabetic patients presents as either confluent or highly discrete white matter abnormalities. Ischaemic white matter lesions are located more peripherally than typical MS plaques and only very rarely do they involve the corpus callosum, dorsal brainstem or cerebellar peduncles. Discrete abnormalities within the ventral pons, basal ganglia and thalami that have low T1W and high T2W signal on MRI are consistent with small vessel infarcts. (Chapman, 2003)

B. **Vasculitis**— imaging appearances are entirely non-specific and range from extensive confluent abnormalities to focal white matter lesions. Catheter angiography may demonstrate segmental irregularity and/or occlusion. (Chapman, 2003)

2.7.Texture Analysis:

Texture can be defined as the relationship between the pixels; therefore it can pick up the microscopic structures and hence it is superior to visual perception which is solely subjective. Texture can be calculate using a window of appropriate size that depict the underlined textures using features vector that correlated with the classes of interest for successful classification and segmentation of the underline textures through a suitable classifier (e.g. k-means, linear discriminate analysis, neural net work etc…).Texture is an important characteristic for the analysis of many types of images. It can be seen in all images from multi spectral scanner images obtained from aircraft or satellite platforms (which the remote sensing community analyzes) to microscopic images of cell cultures or tissue samples (which the biomedical community analyzes).

Despite its importance and ubiquity in image data, a formal approach or precise definition of texture does not exist. (Haralick, 1979) .

Image texture, defined as a function of the spatial variation in pixel intensities (gray values), is useful in a variety of applications and has been a subject of intense study by many researchers. One immediate application of image texture is the recognition of image regions using texture properties. Texture is the most important visual cue in identifying these types of homogeneous regions. This is called texture classification. (Haralick, 1979)

Image analysis techniques have played an important role in several medical applications. In general, the applications involve the automatic extraction of features from the image which is then used for a variety of classification tasks, such as distinguishing normal tissue from abnormal tissue. Depending upon the particular classification task, the extracted features capture morphological

properties, color properties, or certain textural properties of the image. (Clausi et. al., 2002)

Texture is a combination of repeated patterns with a regular frequency. In visual interpretation texture has several types, for example, smooth, fine, coarse etc., which are often used in the classification of forest types. Texture analysis is can also be defined as the classification or segmentation of textural features with respect to the shape of a small element, density and direction of regularity. In the case of digital image, it is difficult to treat the texture mathematically because texture cannot be standardized quantitatively and the data volume is so huge. (Clausi et. al., 2002)

2.7.1 Texture Analysis Types:

Approaches to texture analysis are usually categorized into:

Structural,

Statistical,

Model-based and

Transform.(Materka, 1998)

2.7.2 .Feature Estimation

Numerous approaches to the quantification and characterization of image texture have been proposed, with most textural features falling under 3 general categories: syntactic, statistical, and spectral. (Kassner, 2010)

2.7.2.1. Syntactic texture:

analysis identifies fundamentalor "primitive" elements of the image, which are then linked through syntax. Although it appears to show potential for brain surface mapping and volumetry, to the best of our knowledge, there have been very few

reported applications of syntactic texture analysis to neuro-MR imaging.(Kassner, 2010)

2.7.2.2. Statistical Features:

Statistical approaches do not attempt to understand explicitly the hierarchical structure of the texture. Instead, they represent the texture indirectly by the non-deterministic properties that govern the distributions and relationships between the grey levels of an image. Methods based on second-order statistics (i.e. statistics given by pairs of pixels) have been shown to achieve higher discrimination rates than the power spectrum (transform-based) and structural methods. Human texture discrimination in terms of texture statistical properties is investigated in. Accordingly, the textures in grey-level images are discriminated spontaneously only if they differ in second order moments. Equal second order moments, but different third-order moments require deliberate cognitive effort. This may be an indication that also for automatic processing, statistics up to the second order may be most important. The most popular second-order statistical features for texture analysis are derived from the so-called co-occurrence matrix. They were demonstrated to feature a potential for effective texture discrimination in biomedical-images. The approach based on multidimensional co-occurrence matrices was recently shown to outperform wavelet packets (a transform-based technique) when applied to texture classification. (Materka, 1998)

2.7.2.3. Spectral Features:

Co-occurrence or run-length features may lack the sensitivity to identify larger scale or more coarse changes in spatial frequency. Wavelet functions, for example, can be designed to evaluate spatial frequencies at multiple scales and have found a natural application to texture analysis. Readers will recognize the close relative of the wavelet transform, the Fourier transform, which can identify the spatial frequencies present in a signal intensity but cannot delineate temporal changes in

frequency content and presumes that all signals reflect a superposition of sinusoids. Sometime localization can be imparted to Fourier analysis by means of the windowed or "short-time" method, which allows for the Fourier transform to be performed on sequential portions of the entire signal intensity, each of a set length or "window."The wavelet transform provides even more flexibility by enabling us to trade some degree of spatial-frequency resolution for the ability to localize this frequency content in time. (Kassner, 2010)

2.8. Previous Studies:

- Zhang J, et al (2008) In there study, texture analysis was performed on MR images of MS patients and normal controls and a combined set of texture features were explored in order to better discriminate tissues between MS lesions, normal appearing white matter (NAWM) and normal white matter (NWM). Features were extracted from gradient matrix, run-length matrix, gray level co-occurrence matrix (GLCM), autoregressive model and wavelet analysis, and were selected based on greatest difference between different tissue types. The results of this study demonstrated that (1) with the combined set of texture features, classification was perfect (100%) between MS lesions and NAWM (or NWM), less successful (88.89%) among the three tissue types and worst (58.33%) between NAWM and NWM; (2) compared with GLCM-based features, the combined set of texture features were better at discriminating MS lesions and NWM, equally good at discriminating MS lesions and NAWM and at all three tissue types, but less effective in classification between NAWM and NWM. This study suggested that texture analysis with the combined set of texture features may be equally good or more advantageous than the commonly used GLCM-based features alone in discriminating MS lesions and NWM/NAWM and in supporting early diagnosis of MS.

- Theocharakis P, et al (2009) in their study a pattern recognition system has been developed for the discrimination of multiple sclerosis (MS) from cerebral micro-angiopathy (CM) lesions based on computer-assisted texture analysis of magnetic resonance images. Twenty-three textural features were calculated from MS and CM regions of interest, delineated by experienced radiologists on fluid attenuated inversion recovery images and obtained from 11 patients diagnosed with clinically definite MS and from 18 patients diagnosed with clinically definite CM. The probabilistic neural network classifier was used to construct the proposed pattern recognition system and the generalization of the system to unseen data was evaluated using an external cross validation process. According to the findings of the present study, statistically significant differences exist in the values of the textural features between CM and MS: MS regions were darker, of higher contrast, less homogeneous and rougher as compared to CM.

- Zhang et al (2007) The aim of their study was to investigate the performance of texture analysis in texture classification and tissue discrimination between MS lesions, normal appearing white matter (NAWM) and normal white matter (NWM) in order to support early diagnosis of MS. T2-weighted MR images of sixteen relapsing remitting MS patients and sixteen healthy subjects were selected. Based on the lesion size, sixteen regions of interests (ROIs) were chosen from MS patient MR images and healthy subject MR images for MS lesions, NAWM and NWM respectively. Texture features extracted from grey level co-occurrence matrix (GLCM) were selected based on greatest feature difference. For statistical analysis, raw data analysis (RDA), principal component analysis and nonlinear discriminant analysis (NDA) were applied to the texture features. The k-nearest neighbor and artificial neural network methods were used for texture classification. Fisher coefficient and classification accuracy were used to evaluate the performance of

texture analysis. The results demonstrated that (1) classification was successful (>90.00%) between MS lesions and NAWM or NWM, less successful (88.89%) among the three tissue groups and worst (66.67%) between NAWM and NWM; (2) In statistical analysis, NDA outperforms RDA and principal component analysis; (3) artificial neural network classified more accurately than k-nearest neighbor method between NAWM and NWM, and among the three texture types. This study demonstrated that MRI texture analysis can achieve high classification accuracy in tissue discrimination between MS lesions and NAWM or NWM, which is valuable in supporting early diagnosis of MS.

- Michoux et al (2015), studied the evaluation of the performance of an alternative model assessing the inflammatory activity of MS lesions by texture analysis of T2-weighted MR images. Brain blood barrier breakdown as assessed by contrast-enhanced (CE) T1-weighted MR imaging is currently the standard radiological marker of inflammatory activity in multiple sclerosis (MS) patients. Twenty-one patients with definite MS were examined on the same 3.0 T MR system by T2-weighted, FLAIR, diffusion-weighted and CE-T1 sequences. Lesions and mirrored contralateral areas within the normal appearing white matter (NAWM) were characterized by texture parameters computed from the gray level co-occurrence and run length matrices, and by the apparent diffusion coefficient . Statistical differences between MS lesions and NAWM were analyzed. ROC analysis and leave-one-out cross-validation were performed to evaluate the performance of individual parameters, and multi-parametric models using linear discriminant analysis (LDA), partial least squares and logistic regression in the identification of CE lesions. apparent diffusion coefficient, and all but one texture parameter were significantly different within white matter lesions compared to within NAWM (p < 0.0167). Using LDA, an 8-texture parameter model identified CE lesions with a

sensitivity Se = 70% and a specificity Sp = 76%. Using logistic regression, a 10-texture parameter model performed better with Se = 86%/ Sp = 84%. Using partial least squares, a 6-texture parameter model achieved the highest accuracy with Se = 88%/ Sp = 81%. Texture parameter from T2-weighted images can assess brain inflammatory activity with sufficient accuracy to be considered as a potential alternative to enhancement on CE T1-weighted images.

- Loizou C, et al (2009) The objective of their work was to investigate six different MRI intensity normalization methods and propose the most appropriate for the pre-processing of brain T2-weighted MR images acquired from 22 symptomatic untreated multiple sclerosis (MS) subjects and 10 healthy volunteers. image intensity normalization methods first be applied to magnetic resonance (MR) images to further image analysis. Following image normalization, texture analysis was carried out in original and normalized images for normal appearing white matter (NAMW) and MS lesions, detected in transverse T2-weighted MR images. The best normalization method (Histogram Normalization (HN)) demonstrated a smaller Kullback Leibler divergence (0.05, 0.06) suggesting appropriateness for pre-processing MR images used in texture analysis of MS brain lesions.

-Yu O, et al (1999) studied the distinct patterns of active and non-active plaques using texture analysis on brain MR images in multiple sclerosis patients . Out of thirty-two lesions identified in eight MS patients, nine were considered active, judging from their gadolinium uptake. Using discriminant analysis allowed to classify the lesions into two groups: active or non-active. An attempt to classify their level of activity by using only co-occurrence matrices was unsuccessful. Alternately, the same type of analysis performed on run length analysis criteria allowed the accurate classification of 88% of active lesions and 96% of non-active lesions. Using incremental discriminate analysis can reduce the number of useful

parameters. This method showed that among the 42 parameter , 8 only were highly significant and permitted an accurate classification. Five of these parameters are run length parameters, and three others are more directly related to the global distribution. The main interest of runlength parameters is that they allowed to demonstrate that the lesion structure was different in active and non-active plaques.

- Johnston B, et al (1996) studied the segmentation of brain tissues in magnetic resonance images of the brain, they have implemented a stochastic relaxation method which utilizes partial volume analysis for every brain voxel, and operates on fully three-dimensional (3-D) data. To improve lesion segmentation the authors have extended their method of stochastic relaxation by both pre- and post-processing the MR images. The preprocessing step involves image enhancement using homo-morphic filtering to correct for non-homogeneities in the coil and magnet. Because approximately 95% of all multiple sclerosis lesions occur in the white matter of the brain, the post-processing step involves application of morphological processing and thresholding techniques to the intermediate segmentation in order to develop a mask image containing only white matter and Multiple Sclerosis (MS) lesion. This white/lesion masked image is then segmented by again applying the authors' stochastic relaxation technique. The process has been applied to multispectral MRI scans of multiple sclerosis patients and the results compare favorably to manual segmentations of the same scans obtained independently by radiology health professionals.

- Harrison L, (2010) studied MRI texture analysis in multiple sclerosis . Their intention was to show which parts of the analysis are sensitive to slight changes in textural data acquisition and which steps tolerate interference. They used MRI datasets of 38 multiple sclerosis patients were used in this study. Three imaging sequences were compared in quantitative analyses, including a comparison of

anatomical levels of interest, variance between sequential slices and two methods of region of interest drawing. They focused on the classification of white matter and multiple sclerosis lesions in determining the discriminatory power of textural parameters. Analyses were run with MaZda software for texture analysis, and statistical tests were performed for raw parameters. And found that MRI texture analysis based on statistical, autoregressive-model and wavelet-derived texture parameters provided an excellent distinction between the image regions corresponding to multiple sclerosis plaques and white matter or normal-appearing white matter with high accuracy (nonlinear discriminant analysis 96%–100%). There were no significant differences in the classification results between imaging sequences or between anatomical levels. Standardized regions of interest were tolerant of changes within an anatomical level when intra-tissue variance was tested.

- Ghazel et al (2006) In this work, they propose a semi-automated MS lesion detection system that combines the knowledge of the expert with the computational capacity to produce faster and more reliable MS segmentation results. In particular, the user selects coarse regions of interest (ROIs) that may potentially contain MS lesions. Then any MS lesions within the provided ROI's are then detected and segmented based on texture analysis. The method is applied on real MRI data and the results are qualitatively compared to a ground truth, which is manually segmented by a human expert. However, these automated methods generally produce segmentation results that agree only partially with the ground truth segmentation provided by the experts. They also suffer from miss-classification errors, especially false-negative miss-classification where true lesions are left undetected, which is a grave concern from a medical point of view.
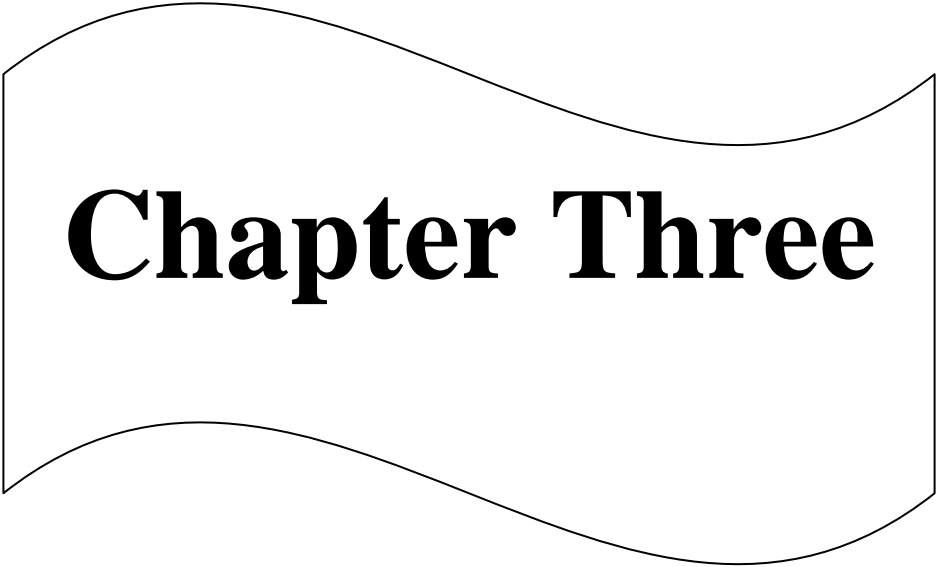
Chapter Three

Chapter Three
Materials and Methods

3.1. Study design:

This is analytical study of a case control type where normal MR images of the brain were taken as a reference.

3.2. Study population:

The population of this study included patients having multiple sclerosis and patients having small vascular desease and have done MRI .

3.3. Study area and duration:

This study had been achieved in Antalia hospital (GE 1.5 T MRI machine) and it was conducted from September 2016 to December 2016

3.4. Sample size and type:

The sample of this study was consisted from 50 MR brain (FLAIR and T2) images selected conveniently from patient with MS and 50 MR brain FLAIR images from patient with SVD .

3.5. Method of data collection and analysis:

After that MR image were stored in computer disk they was viewed by the Radiant, Ant . DICOM in computer to select the section of image and uploaded it into the computer based software Interactive Data language (IDL) where the DICOM image converted to TIFF format and the user then clicks on areas represents the gray matter, white matter, CSF and MS plaque . In these areas a window of 3×3 pixel will be set and the first order statistics were calculated, which

include mean , SD , energy and entropy . These features are then assigned as classification center used to classify the whole image into different classes using the Euclidean distance. The algorithm scans the whole image using a window of 3×3pixel and computes the first order statistics and computes the distance (the Euclidean distance) between the calculated features and the class's centers and assigns the window to the class with the lowest distance. Then the window interlaced one pixel and the same process stated over till the entire image were classified the data concerning the gray matter, white matter and MS plaque will then be entered into SPSS with its classes to generate a classification score using stepwise linear discriminate analysis; to select the most discriminate feature that can be used in the classification of normal and abnormal brain tissues . then scatter plot using discriminate function is generated as well as classification accuracy and linear discriminate function equation to differentiate between normal and abnormal brain tissue for unseen images.

3.6. Ethical approval:

Ethical approval is granted from Antalia hospital where no patient identification data or individual patient detail is published.
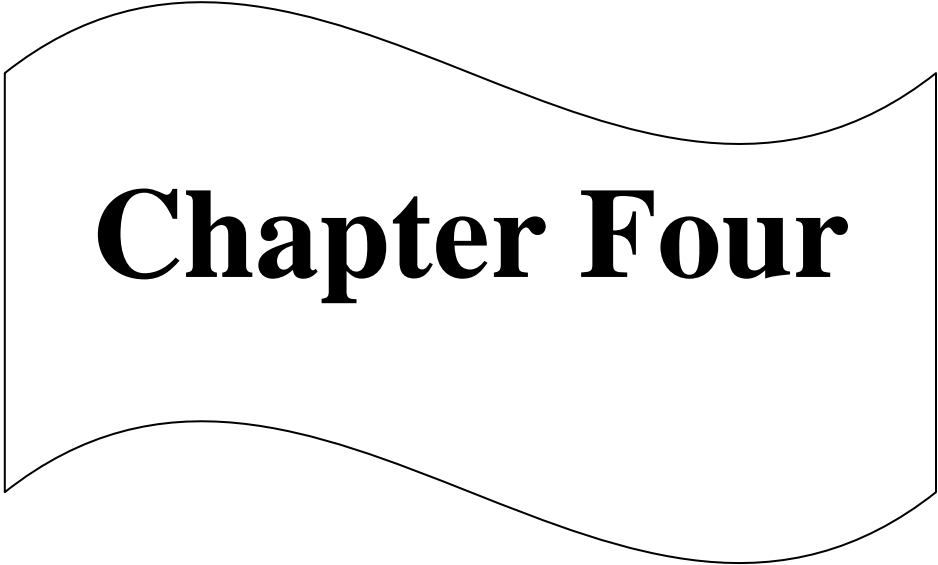
Chapter Four

Chapter four

Results
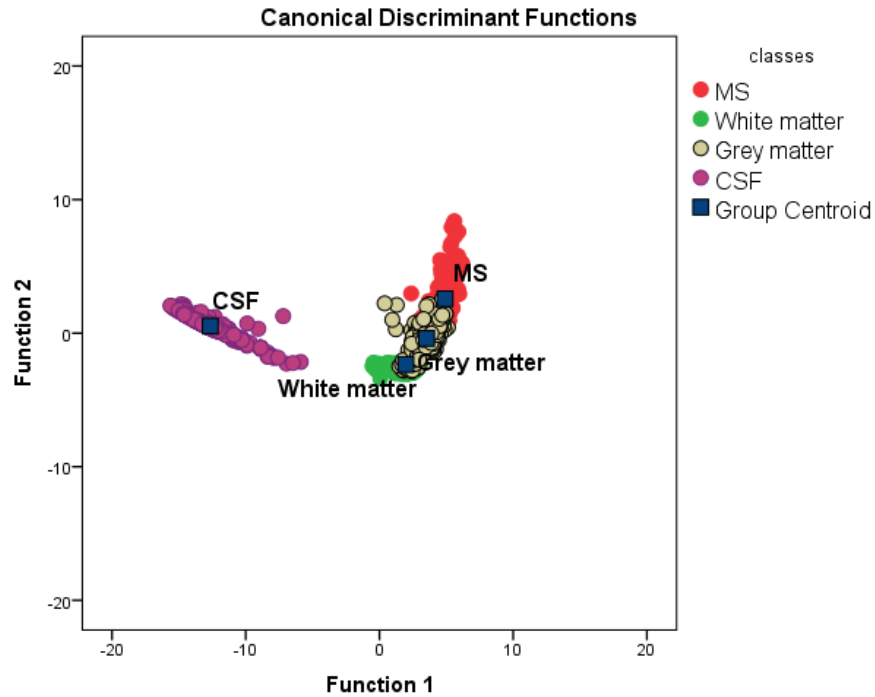
Fig 4-1: Scatter plot show the classification of brain tissues using linear discriminate analysis on FLAIR images for MS patients
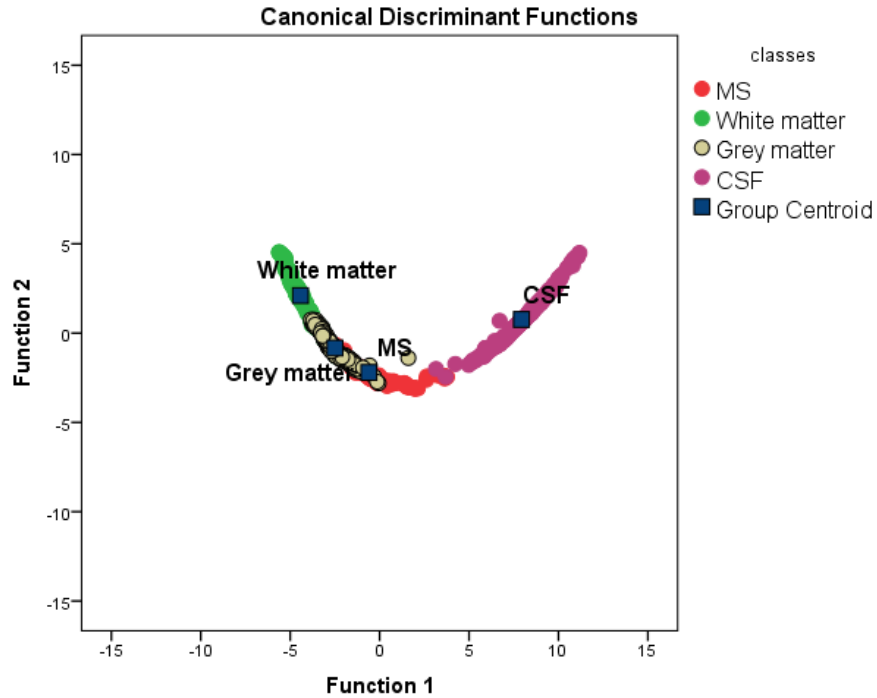
Table 4-1: Cross-tabulation table show the classification results tissues using linear discriminate analysis on FLAIR images for MS patients

Classes		Predicted Group Membership				Total
		MS	White matter	Grey matter	CSF	
Original	MS	85.6	0.0	14.4	0.0	100.0%
	White matter	0.0	94.2	5.8	0.0	100.0%
	Grey matter	4.3	10.5	85.2	0.0	100.0%
	CSF	0.0	0.0	0.0	100.0	100.0%

Sensitivity =85.6%

Specificity = 93.1%

Accuracy =91.2%

Fig 4-2: Scatter plot show the classification of brain tissues using linear discriminate analysis onT2 images for MS patients

Table 4-2: Cross-tabulation table show the classification results tissues using linear discriminate analysis on FLAIR images for MS patients

Classes		Predicted Group Membership				Total
		MS	White matter	Grey matter	CSF	
Original	MS	91.1	0.0	8.9	0.0	100.0%
	White matter	.3	85.3	14.4	0.0	100.0%
	Grey matter	15.4	2.6	82.0	0.0	100.0%
	CSF	.6	0.0	0.0	99.4	100.0%

Sensitivity = 91.1 %

Specificity = 88.9 %

Accuracy = 89.5 %
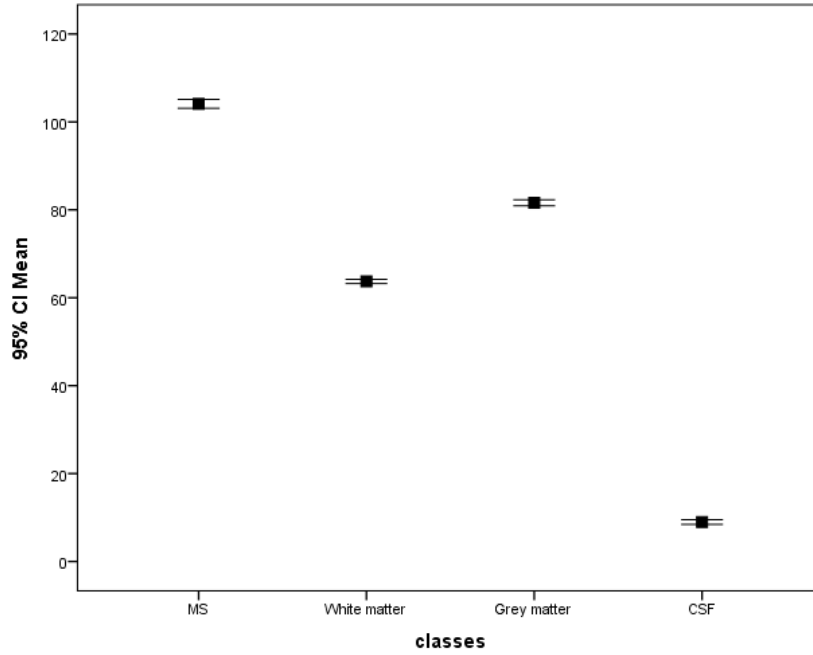
Fig 4-3: Error bar plot show the discriminate power of the mean textural feature distribution for the selected classes on FLAIR images for MS patients
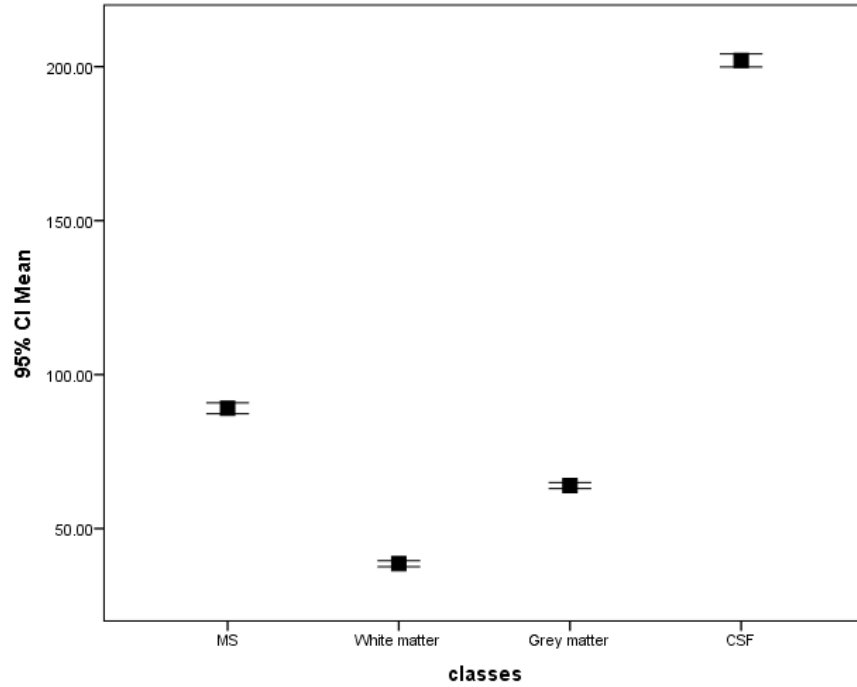
Fig 4-4: Error bar plot show the discriminate power of the mean textural feature distribution for the selected classes on T2 images for MS patients
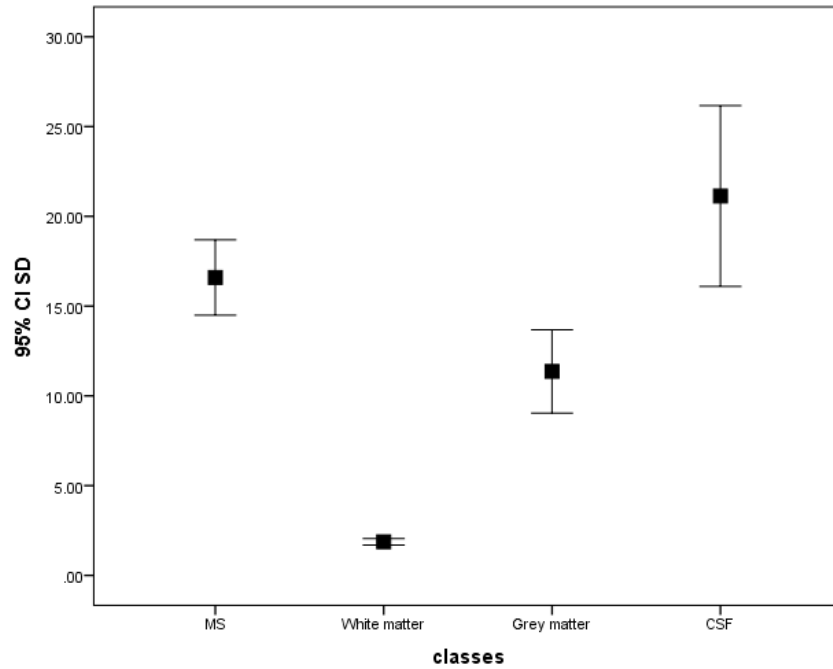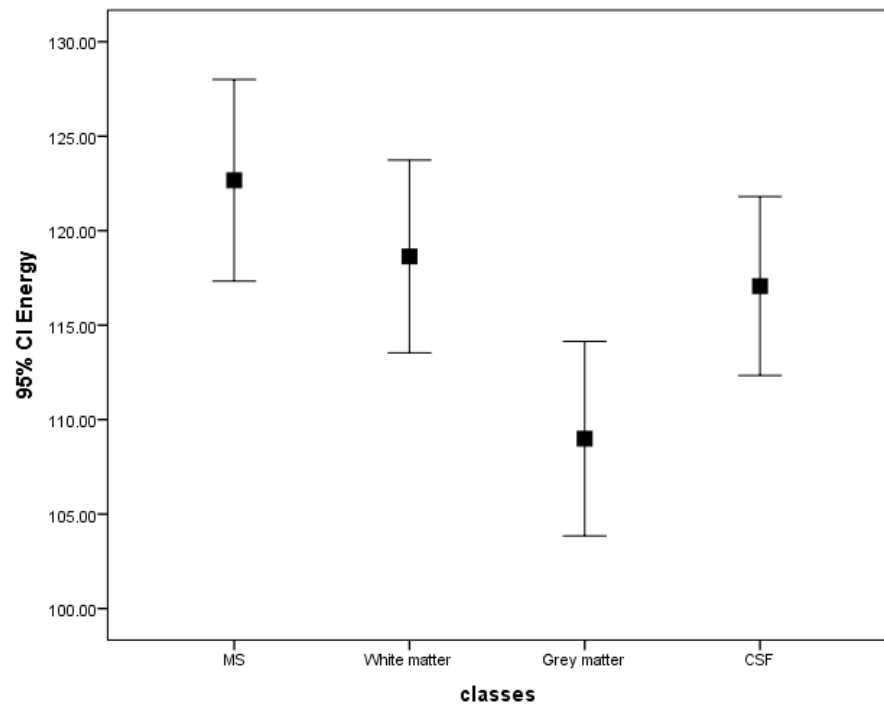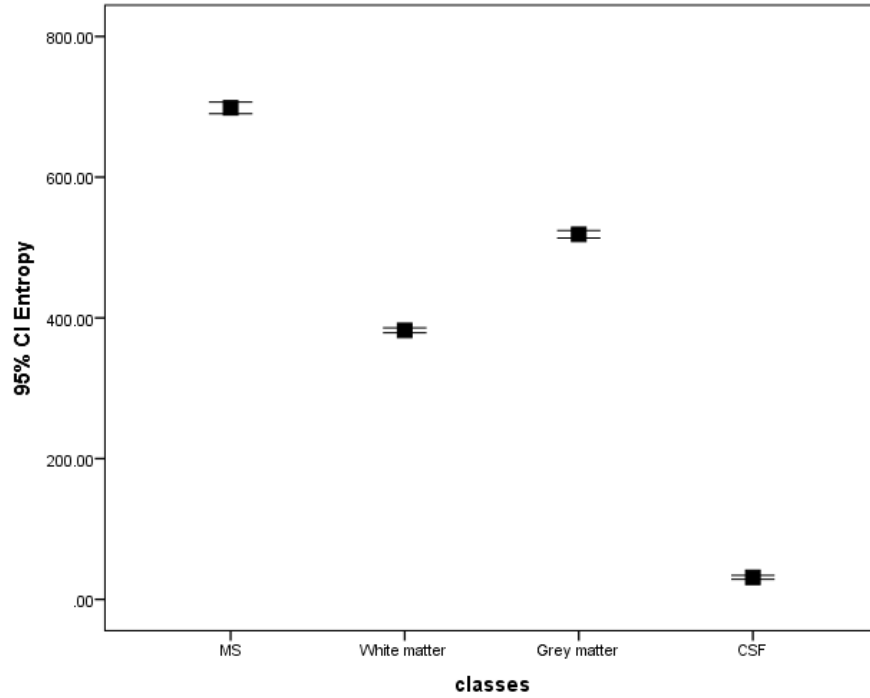
Fig 4-5: Error bar plot show the discriminate power of the Stander Deviation textural feature distribution for the selected classes on FLAIR images for MS patients
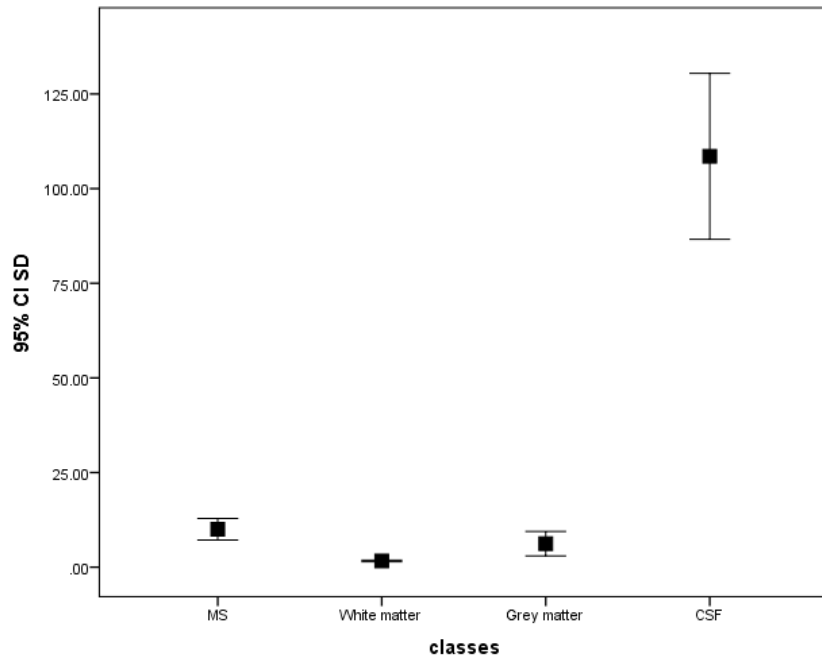
Fig 4-6: Error bar plot show the discriminate power of the Stander Deviation textural feature distribution for the selected classes on T2 images for MS patients
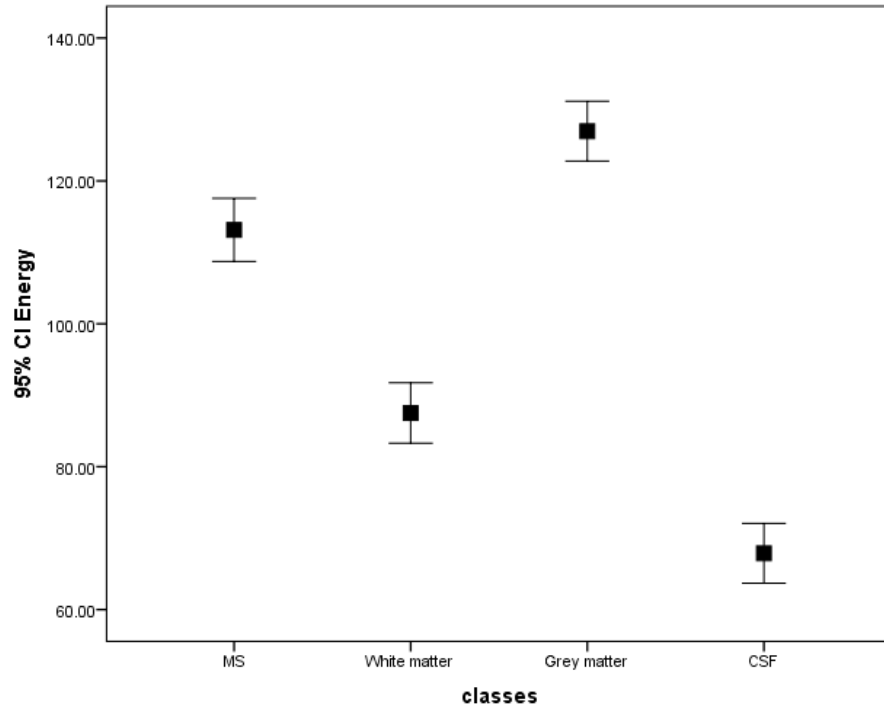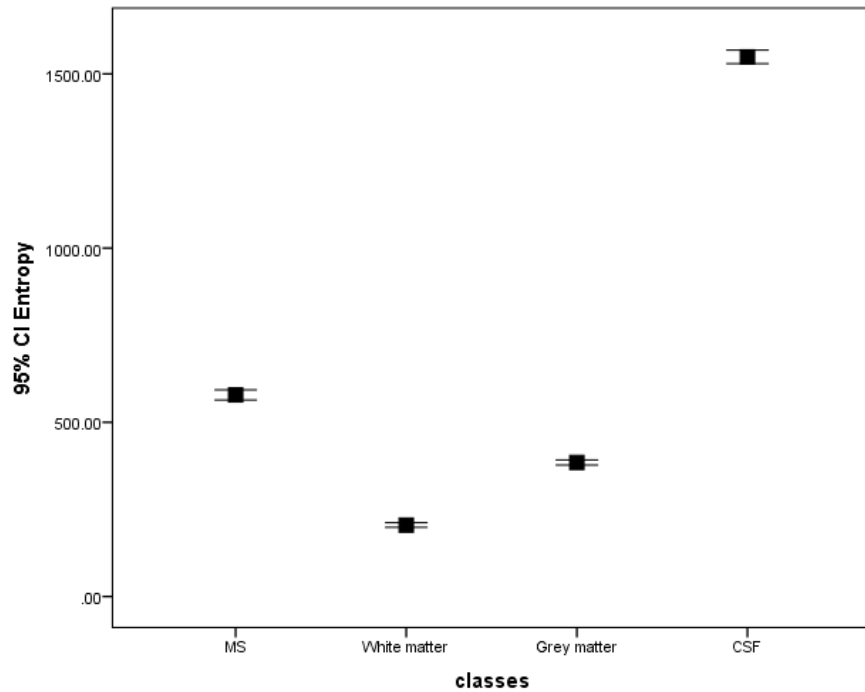
Fig 4-7: Error bar plot show the discriminate power of the energy textural feature distribution for the selected classes on FLAIR images for MS patients


Fig 4-8: Error bar plot show the discriminate power of the energy textural feature distribution for the selected classes on T2 images for MS patients

Fig 4-9: Error bar plot show the discriminate power of the Entropy textural feature distribution for the selected classes on FLAIR images for MS patients
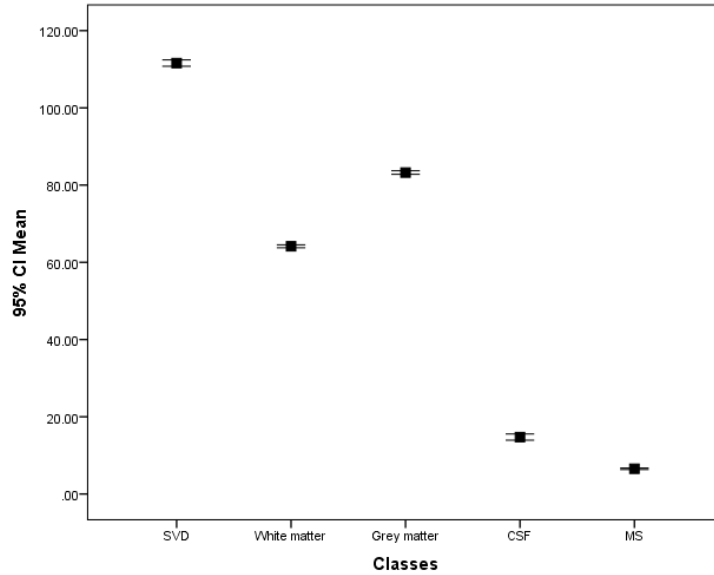

Fig 4-10: Error bar plot show the discriminate power of the Entropy textural feature distribution for the selected classes on T2 images for MS patients
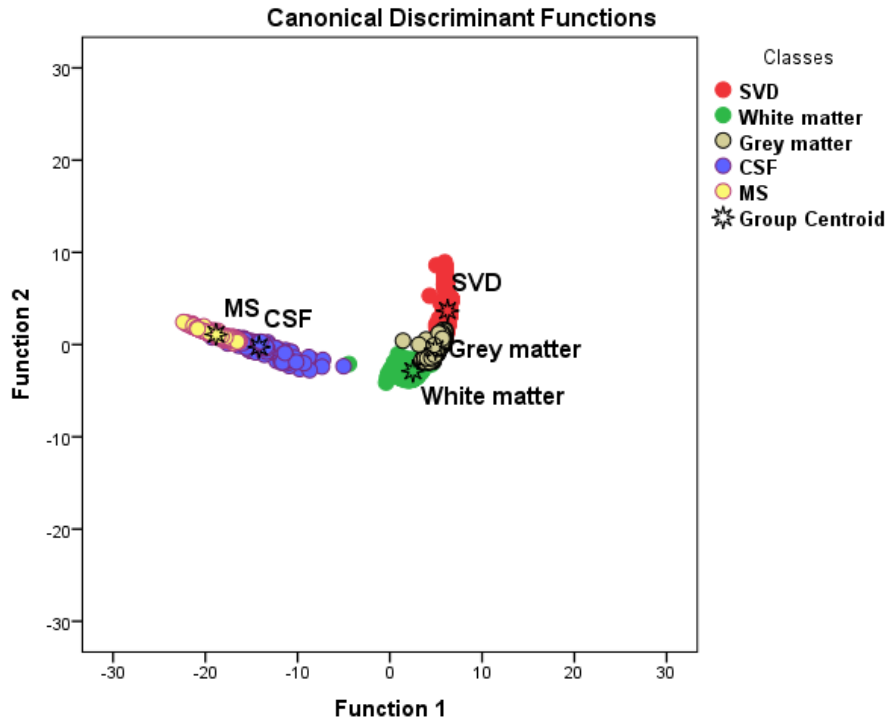
Fig 4-11: Scatter plot show the classification of brain tissues using linear discriminate analysis on FLAIR images for SVD & MS patients

Table 4-3: Cross-tabulation table show the classification results tissues using linear discriminate analysis on FLAIR images for SVD & MS patients

| Classes		Predicted Group Membership					Total
		SVD	White matter	Grey matter	CSF	MS	
Original	SVD	92.6	0.0	7.4	0.0	0.0	100.0%
	White matter	0.0	100.0	0.0	0.0	0.0	100.0%
	Grey matter	0.0	.7	99.3	0.0	0.0	100.0%
	CSF	0.0	.5	0.0	94.5	5.1	100.0%
	MS	0.0	0.0	0.0	1.5	98.5	100.0%

49

Fig 4-12: Error bar plot show the discriminate power of the mean textural feature distribution for the selected classes on FLAIR images for both MS & SVD patients
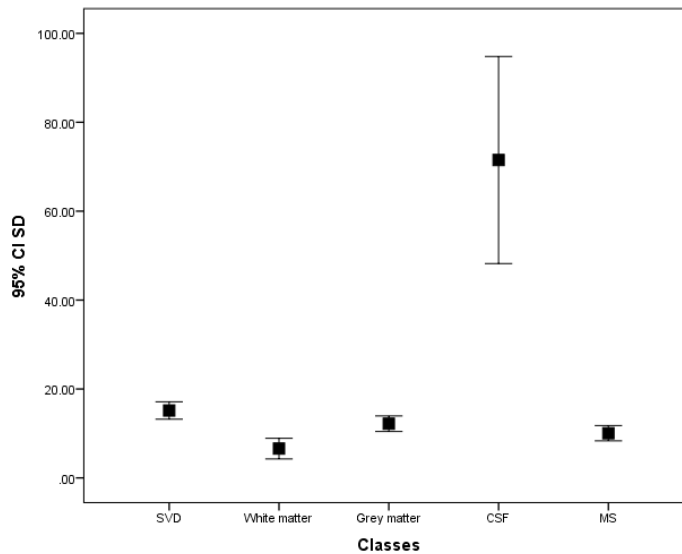

Fig 4-13: Error bar plot show the discriminate power of the SD textural feature distribution for the selected classes on FLAIR images for both MS & SVD patients
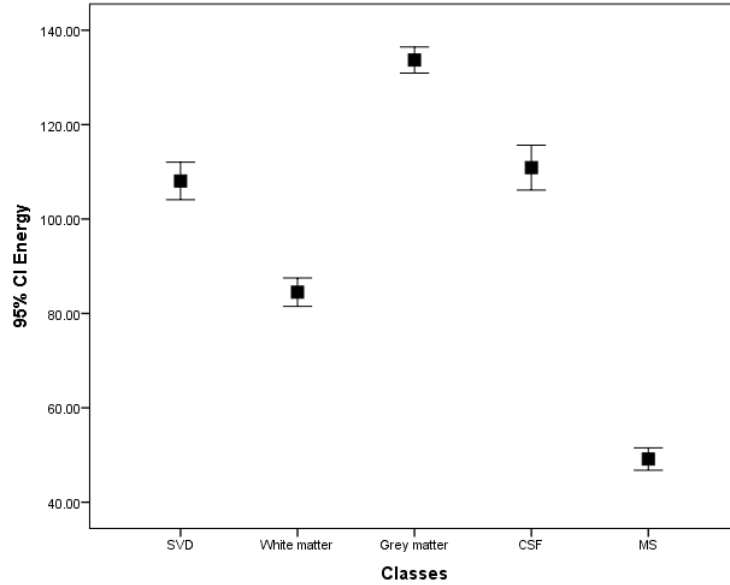
Fig 4-14: Error bar plot show the discriminate power of the energy textural feature distribution for the selected classes on FLAIR images for both MS & SVD patients
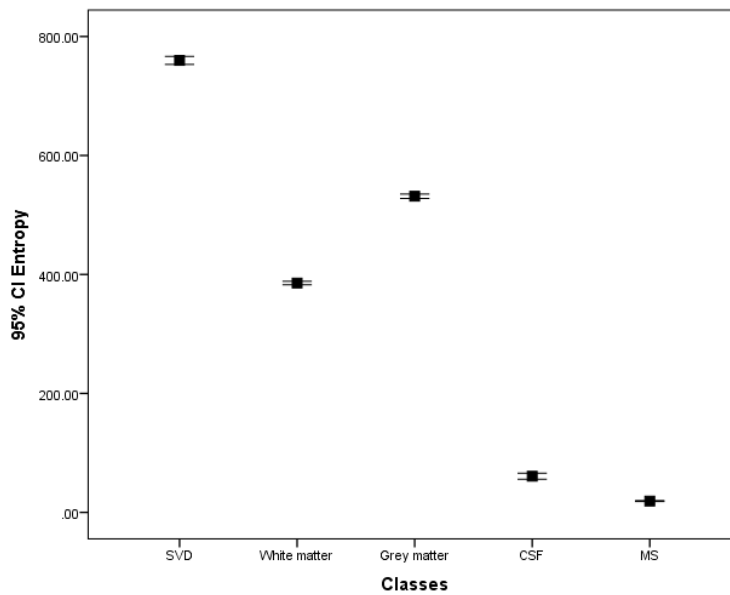
Fig 4 -15: Error bar plot show the discriminate power of the entropy textural feature distribution for the selected classes on FLAIR images for both MS & SVD patients
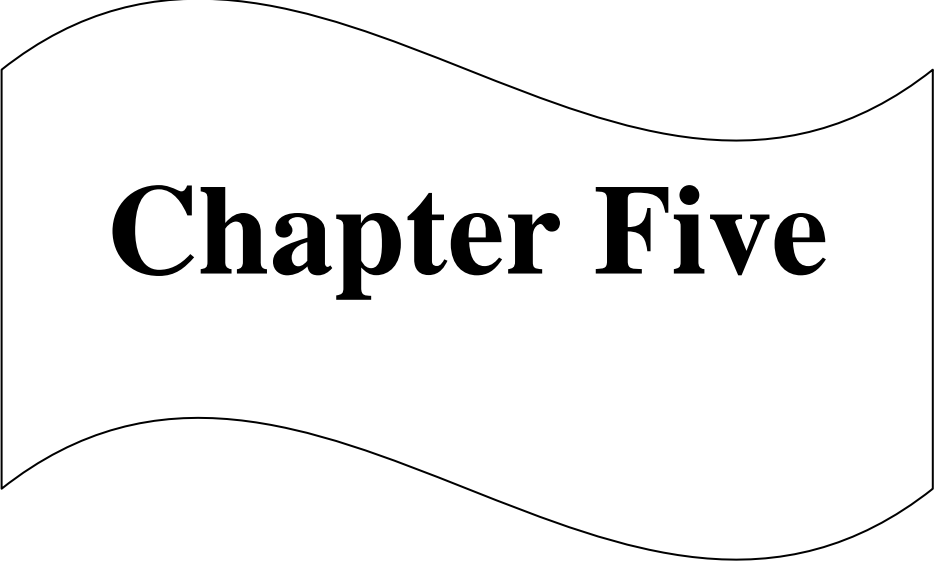
Chapter Five

Chapter five

Discussion, conclusion and Recommendation

The main aim of this study was to classify the brain tissues in MR images into normal tissues and MS plaques using Texture analysis features

5.1. Discussion:

In this study there were four features extracted from the gray matter, white matter, CSF and MS plaque using window of 3×3 pixel. From these four features showed significant correlation with the perdifind classes (gray matter, white matter, CSF and MS plaque) they includes the mean , SD , energy and entropy.

To classify brain tissue to normal and abnormal (MS) using linear discriminate analysis . the result of classification showed that MS areas were very different from the rest of the tissues on FLAIR **Fig4-1** and T2 **Fig 4-2** images with classification accuracy of 91.2% , sensitivity = 85.6% and specificity = 93.1% on FLAIR images **Table 4-1** and classification accuracy of 89.5 % , sensitivity = 91.1% and specificity = 88.9% on T2 images **Table 4-2.**

From **Fig 4-3**&**Fig 4-4** on FLAIR images the MS plaques has the highest mean than the rest of brain tissue but on T2 images the signal of CSF had the highest mean then come the MS becouse fluid signal is not attenuated. Also when use SD feature had discriminat better on T2 images (between the MS and Gray matter) but on FLAIR there is interferans btween the classis (between the MS , Gray matter and CSF) (**Fig 4-5**&**Fig 4-6**) .

The use of energy textural feature had discreminat between the MS plaques and other brain tissue successfully on FLAIR images but on T2 images there is a interfirence between the MS , white matter and CSF. That means the MS contrast is well difreniated from normal brain tissue on FLAIR images (**Fig 4-7**&**Fig 4-8**).

When use the discreminat power of the entropy textural feature on MS and normal brain tissues on FLAIR and T2 images has successfully differentiate between them on both sequences (**Fig 4-9**&**Fig 4-10**).

As compared to study done by Zhang (2007) he used NDA to classify   between MS and NAWM found the accuracy = 90% but on 2008 when he used LR matrix the accuracy was 100% seam as this study when comparing the MS and the NAWM.

From **Fig 4-11** the result of the classifiction showed that the MS plaques were very different from SVD with classifiction accuracy of 100% between both of them (no inter ferance) on FLAIR images **(Table 4-3).**

 In respect to the applied features the mean ,SD, energy and entropy on FLAIR images can diffrentiate between MS and SVD successfully and the best feature is the entropy followed by mean then energy and the least is SD. And MS regions were darker, and lower contrast as compared to SVD.

  (Fig4-12, 4-13 , 4-14 & 4-15).

5.2. Conclusion:

the aim of this study was to characterize of MS plaques in MR images using Texture analysis features which enabling disease characterization and quantification of disease distribution.

This study is analytical study and had been conducted at Antalia hospital in a period from September 2016 to December 2016 with sample which was consisted from 60 MR brain images for patient having multiple sclerosis.

The result reveals that the MS areas were very different from the rest of the tissues on FLAIR images with classification accuracy of 91.2% and on T2 images with classification accuracy of 89.5%. And classifiction btween the MS plaques and SVD are very different with classifiction accuracy of 100% between both of them (no inter ferance) on FLAIR images

In conclusion MS can be diagnosed objectively by:

*sensitivity equal to 85.6% on FLAIR images using the following equations:

MS = (25.663×mean) + (-.267×SD) + (-.107×energy) + (-3.060×entropy) -260.181
White matter = (26.430×mean) + (-.266×SD) + (-.122×energy) + (-3.261×entropy) -214.736
Grey matter = (26.550×mean) + (-.267×SD) + (-.103×energy) + (-3.232×entropy) -238.124
CSF = (8.120×mean) + (-.047×SD)+ (-.015×energy) + (-1.032×entropy) -20.686

*sensitivity equal to 91.1% on T2 images using the following equations:

MS = (12.262×mean) + (-.008×SD) + (.033×energy) + (-1.412×entropy) -140.994
White matter = (8.580×mean) + (-.008×SD) + (.037×energy) + (-1.003×entropy) -66.398
Grey matter = (11.035×mean) + (-.009×SD) + (.028×energy) + (-1.281×entropy) -109.351
CSF = (10.690×mean) + (.016×SD)+ (.042×energy) + (-1.147×entropy) -196.357

Also SVD can be diagnosed objectively by sensitivity equal to 92.6 % on FLAIR images using the following equation:

SVD = (50.525×mean) + (-.198×SD) + (.062×energy) + (-6.093×entropy) -507.786

5.3. Recommendation:

- Large sample can be used to have better overall accuracy using representative data set.
- Other type of diseases and feature can use or comparison between diseases have the same radiographic appearance.
- IDL program should be adopted by the radiology department to deal with the challenging cases and to have an objective second opinion.
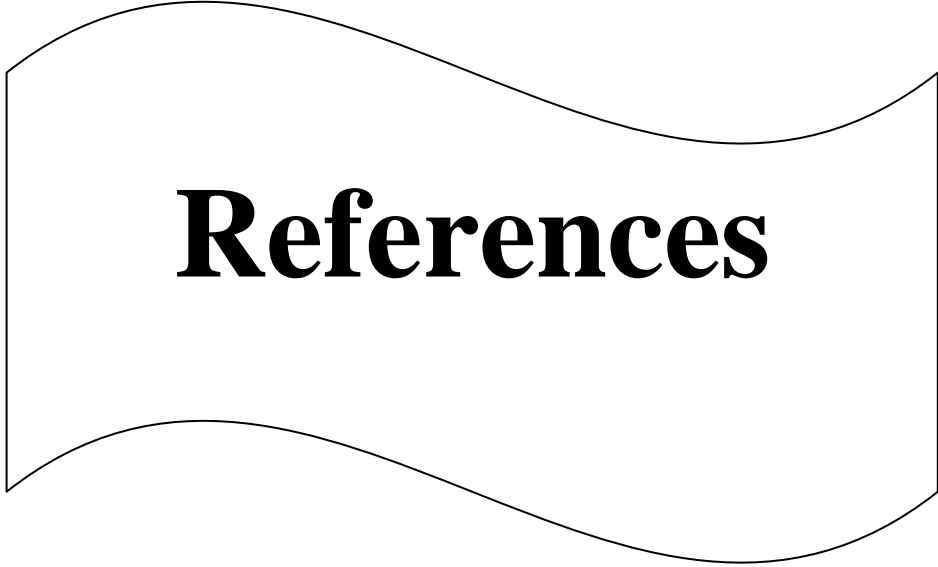
References

References :

Alastair Compston, Alasdair Coles. Multiple sclerosis . The Lancet 2002;VOL 359: 1221–1231

Bontrager .Kenneth L, Lampignano.John P. Textbook Of Radiographic Positioning And Related Anatomy. Eighth Edition. China : Mosby Elsevier Inc 2014.

Chapman .Stephen, Nakielny .Richard. Aids to Radiological Differential Diagnosis . Fourth Edition. London: British Library 2003

Evert J. Blink . MRI Physics. November, 2004 :support@mri-physics.com

Ghazel, Mohsen, Anthony Traboulsee, and Rabab K. Ward. "Semi-automated segmentation of multiple sclerosis lesions in brain MRI using texture analysis."2006 IEEE International Symposium on Signal Processing and Information Technology. IEEE, 2006.

Haralick, R. M. 1979. Statistical and structural approaches to texture. Proceedings on the IEEE (67) 5: 786-803.

Harrison, L. C., Raunio, M., Holli, K. K., Luukkaala, T., Savio, S., Elovaara, I., ... & Dastidar, P. (2010). MRI texture analysis in multiple sclerosis: toward a clinical analysis protocol. Academic radiology, 17(6), 696-707.

Johnston, B., Atkins, M. S., Mackiewich, B., & Anderson, M. (1996). Segmentation of multiple sclerosis lesions in intensity corrected multispectral MRI. IEEE Transactions on Medical Imaging, 15(2), 154-169.

Kassner.A, Thornhill .R.E. Texture Analysis: A Review of Neurologic MR Imaging Applications. AJNR Am J Neuroradiol May 2010 31:809 –816

Kelley L.L., Petersen C.M., Sectional Anatomy for imaging professionals, Second Edition, United States of America, Mosby-Elsevier Inc.2007.

Loizou .C.P, Pantziarisb .M , Seimenis .I & Pattichis .C.S . Brain MR Image Normalization in Texture Analysis of Multiple Sclerosis . 9th International Conference on Information Technology and Applications in Biomedicine, ITAB 2009, Larnaca, Cyprus, 5-7 November 2009 :978-982

Malik.J, Belongie. S, Leungand .Th and Shi .J . Contour and Texture Analysis for Image Segmentation . International Journal of Computer Vision Kluwer Academic Publishers. Manufactured in The Netherlands 2001;vol 43(1): 7–27

Mark A. Brown, Richard C. Semelka . MRI Basic Principles And Applications .Third Edition. Hoboken, New Jersey : A John Wiley & Sons, Inc., Publication 2003

Materka, M. Strzelecki, Texture Analysis Methods – A Review, Technical University of Lodz, Institute of Electronics, COST B11 report, Brussels 1998 Stefanowskiego; 18: 90-924

Michoux .N, Guillet. A, Rommel. D,Mazzamuto. G, Sindic .C, Duprez. T . TextureAnalysis of T2-Weighted MR Images to Assess Acute Inflammation in Brain MS Lesions. PLoS ONE 2015 ;10: 1-13: e0145497. doi:10.1371/journal.pone.0145497

Parris M. Kidd .Multiple Sclerosis, An Autoimmune Inflammatory Disease: Prospects for its Integrative Management. Alternative Medicine Review Thorne Research, Inc.2001; Volume 6: 540-566

Theocharakis, P., Glotsos, D., Kalatzis, I., Kostopoulos, S., Georgiadis, P., Sifaki, K., ... & Nikiforidis, G. (2009). Pattern recognition system for the discrimination

of multiple sclerosis from cerebral microangiopathy lesions based on texture analysis of magnetic resonance images. Magnetic resonance imaging, 27(3), 417-422.

Yu, O., Mauss, Y., Zollner, G., Namer, I. J., & Chambron, J. (1999). Distinct patterns of active and non-active plaques using texture analysis on brain NMR images in multiple sclerosis patients: preliminary results. Magnetic resonance imaging, 17(9), 1261-1267.

Zhang, J., Tong, L., Wang, L., & Li, N. (2008). Texture analysis of multiple sclerosis: a comparative study. Magnetic resonance imaging, 26(8), 1160-1166.

Zhang, Jing, Lei Wang, and Longzheng Tong. "Feature reduction and texture classification in MRI-Texture analysis of multiple sclerosis." Complex Medical Engineering, 2007. CME 2007. IEEE/ICME International Conference on. IEEE, 2007.
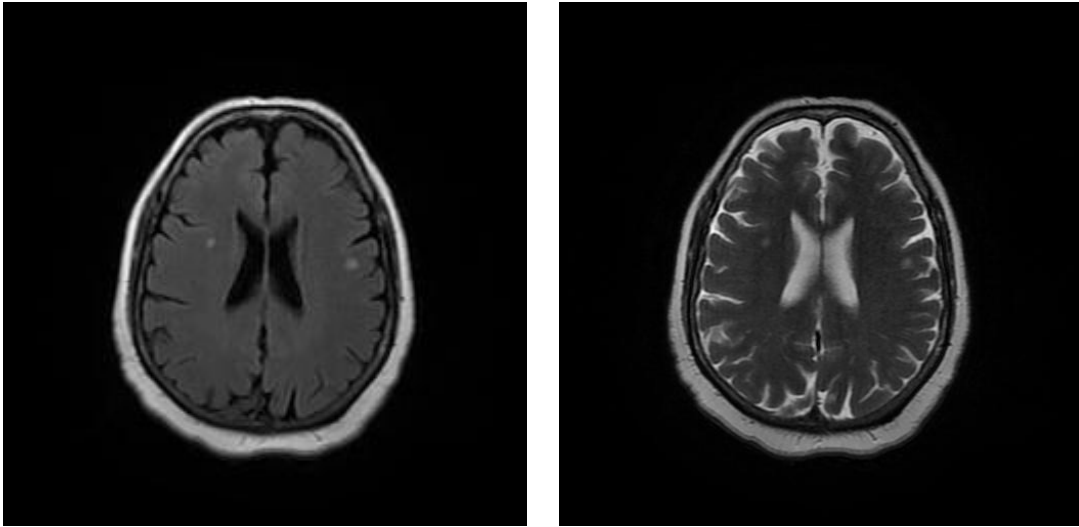
Appendices

Appendix

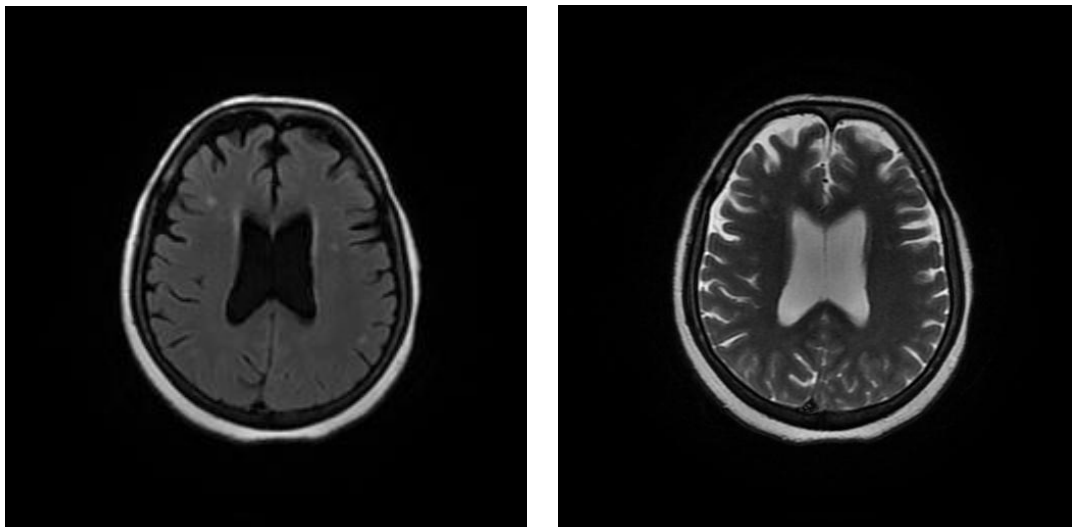Image (A-1): FLAIR & T2 images for patient with MS

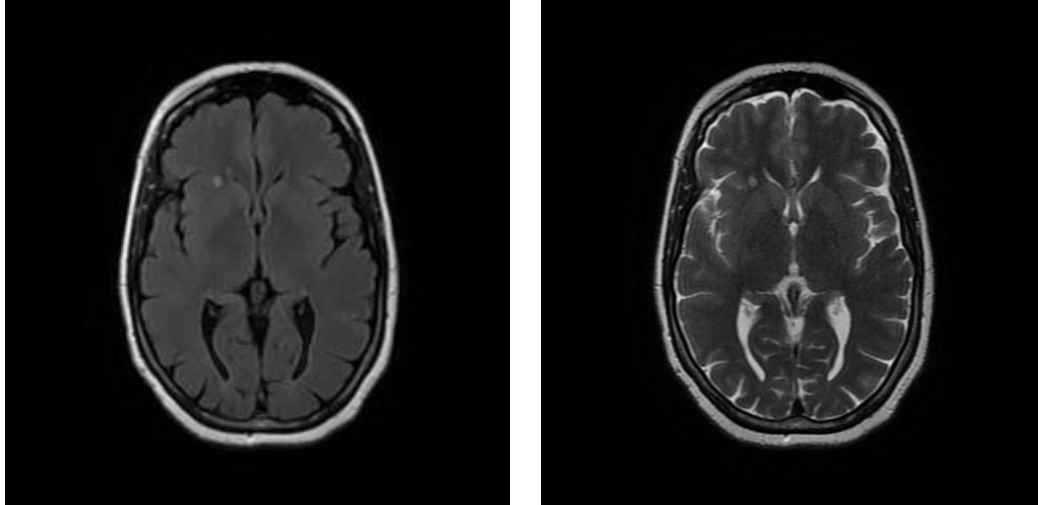Image (A-2): FLAIR & T2 images for patient with MS
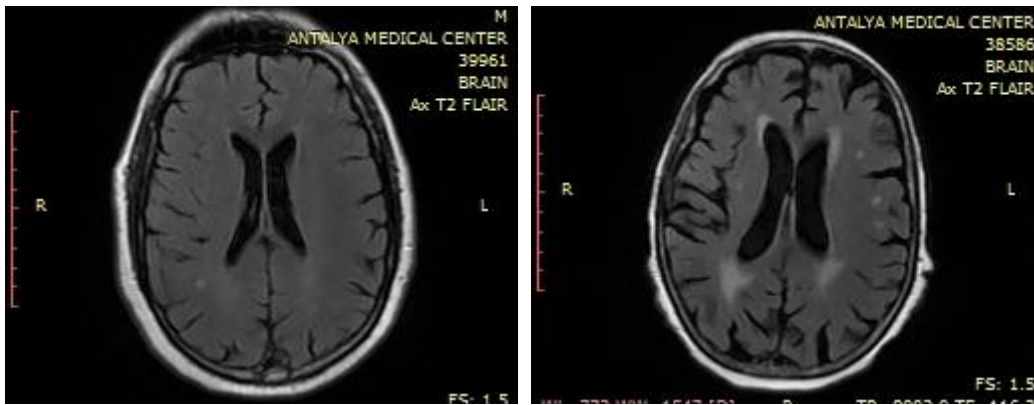
Image (A-3): FLAIR & T2 images for patient with MS

Image (A-4): FLAIR   images for patient with SVD